ANL/NDM-77

A LEAST-SQUARES METHOD FOR DERIVING REACTION DIFFERENTIAL-CROSS-SECTION INFORMATION FROM MEASUREMENTS PERFORMED IN DIVERSE NEUTRON FIELDS*

by

Donald L. Smith

November 1982

Applied Physics Division
Argonne National Laboratory
9700 South Cass Avenue
Argonne, Illinois 60439
USA

NUCLEAR DATA AND MEASUREMENTS SERIES

The Nuclear Data and Measurements Series presents results of studies in the field of microscopic nuclear data. The primary objective is the dissemination of information in the comprehensive form required for nuclear technology applications. This Series is devoted to: a) measured microscopic nuclear parameters, b) experimental techniques and facilities employed in measurements, c) the analysis, correlation and interpretation of nuclear data, and d) the evaluation of nuclear data. Contributions to this Series are reviewed to assure technical competence and, unless otherwise stated, the contents can be formally referenced. This Series does not supplant formal journal publication but it does provide the more extensive information required for technological applications (e.g., tabulated numerical data) in a timely manner.

INFORMATION ABOUT OTHER ISSUES IN THE ANL/NDM SERIES:

A list of titles and authors for reports ANL/NDM-1 through ANL/NDM-50 can be obtained by referring to any report of this series numbered ANL/NDM-51 through ANL/NDM-76. Requests for a complete list of titles or for copies of previous reports should be directed to:

ANL/NDM-51   Measured and Evaluated Neutron Cross Sections of Elemental Bismuth by A. Smith, P. Guenther, D. Smith and J. Whalen, April 1980.

ANL/NDM-52   Neutron Total and Scattering Cross Sections of ^{6}Li in the Few MeV Region by P. Guenther, A. Smith and J. Whalen, February 1980.

ANL/NDM-53   Neutron Source Investigations in Support of the Cross Section Program at the Argonne Fast-Neutron Generator by James W. Meadows and Donald L. Smith, May 1980.

ANL/NDM-54   The Nonelastic-Scattering Cross Sections of Elemental Nickel by A. B. Smith, P. T. Guenther and J. F. Whalen, June 1980.

ANL/NDM-55   Thermal Neutron Calibration of a Tritium Extraction Facility using the ^{6}Li(n,t)^{4}He/^{197}Au(n,γ)^{198}Au Cross Section Ratio for Standardization by M. M. Bretscher and D. L. Smith, August 1980.

ANL/NDM-56   Fast-Neutron Interactions with ^{182}W, ^{184}W and ^{186}W by P. T. Guenther, A. B. Smith and J. F. Whalen, December 1980.

ANL/NDM-57   The Total, Elastic- and Inelastic-Scattering Fast-Neutron Cross Sections of Natural Chromium, Peter T. Guenther, Alan B. Smith and James F. Whalen, January 1981.

ANL/NDM-58   Review of Measurement Techniques for the Neutron Capture Process by W. P. Poenitz, August 1981.

ANL/NDM-59   Review of the Importance of the Neutron Capture Process in Fission Reactors, Wolfgang P. Poenitz, July 1981.

ANL/NDM-60   Neutron Capture Activation Cross Sections of ^{94}Zr, ^{96}Zr, ^{98,100}Mo, and ^{110,114,116}Cd at Thermal and 30 keV Energy, John M. Wyrick and Wolfgang P. Poenitz (to be published).

ANL/NDM-75 Neutron Total and Scattering Cross Sections of Elemental
            Antimony by A. B. Smith, P. T. Guenther, and J. F. Whalen
            (to be published).

ANL/NDM-76 Scattering of Fast-Neutrons from Elemental Molybdenum by
            A. B. Smith and P. T. Guenther (to be published).

TABLE OF CONTENTS

The objective of nuclear data research is acquisition of quantitative knowledge for those nuclear parameters which are important in technological applications. This is a dynamic field because technological requirements continuously change. The investigation of nuclear properties which are not directly related to specific technologies is often required in order to achieve a deeper understanding of certain systematic effects which do impact upon practical applications.

Traditionally, the development of nuclear data information has involved contributions from several distinct subdisciplines. Interaction between researchers examining theoretical and nuclear model problems, nuclear reaction cross section measurers, reactor scientists, evaluators, etc., has been limited. This situation is now changing rapidly. Many of the traditional boundaries between the various facets of nuclear data research have crumbled. Theory and nuclear model calculations have been used by evaluators to develop reasonably reliable evaluations in situations where experimental data are nonexistent or inadequate. Differential cross section measurers have cooperated with integral investigators, thereby eliminating a number of discrepancies which long plagued this field. The roles of experimenter, theorist and evaluator have thus become considerably intermingled. Ambitious programs to develop comprehensive evaluated-data files demand coordinated contributions from all sectors of the nuclear data community in order to satisfy the established goals. This evolution of the field has been a very positive development. Otherwise, it is unlikely that there would have been as much progress as has actually been achieved lately. Clearly, the trend toward amalgamation of the traditional subdisciplines in the nuclear data community has enriched the field and enhanced productivity.

Evaluators have come to recognize that there is no clear boundary between integral and differential data. The terms "differential" and "integral" identify qualitatively whether experiments are performed under narrow-spectrum or broad-spectrum conditions. The distinction is harbored most fervently in the minds of experimentalists whose partisan thinking is strongly influenced by the nature of the facilities where they are employed. Actually, one cannot attribute the development of this artificial distinction entirely to the limitations of research facilities. A researcher who utilizes a filtered beam from a reactor for measurements is effectively a "differentialist." A worker at a Van de Graaff facility who bombards thick targets with high-energy light charged particles can produce very broad neutron spectra indeed, and use them productively for "integral" studies. Investigators who use linac neutron sources can pursue both "differential" and "integral" studies, depending upon the manner in which they utilize the time-of-flight information available to them. Also, we should not forget the contributions from those researchers who utilize radioactive neutron sources such as Ra-Be or Cf-252. Their research encompasses the entire range between "differential" and "integral" methods.

The present work offers what is hoped to be a constructive assault against two traditional boundaries in the nuclear data field, namely integral versus differential and measurement versus evaluation. A method is suggested for addressing the problem of improving knowledge of a specific energy-dependent

reaction cross section, $\sigma(E)$. This method is founded upon the well-known Bayesian approach utilized by evaluators, whereby a prior evaluation of the cross section is "refined" by the addition of new experimental information which is, hopefully, independent of the prior evaluation. What is suggested here is that the researcher can, if he chooses, abandon the traditional approach of restricting a specific investigation to either a differential method which seeks to measure energy-dependent cross sections or an integral method which has the goal of measuring a specific spectrum-average cross section. Instead, he is free to use almost any method for neutron production available at his laboratory in order to measure a set of distinct reaction yields. The researcher then analyzes his results in the context of all prior information, thereby assuming the role of an evaluator. An unbiased, generalized least-squares algorithm which can be used for performing this evaluation task is described in the present report. The researcher who follows this approach thus cannot be identified specifically as a differential or integral measurer, or evaluator. The measured results he reports may not actually be cross sections, yet knowledge of this information could help significantly to refine our knowledge of a specific cross section. Furthermore, the proposed algorithm permits a quantitative assessment of the extent to which the specific new information has improved our knowledge of the cross section.

There are limitations to the method and risks associated with it. For example, if the apriori knowledge is truly wrong, and is too heavily weighted by unrealistically small uncertainties, then the benefits of new information may not be adequately realized. However, the least-squares algorithm has a built-in warning device to signal the existence of such situations. There is the risk associated with an obvious loss of distinction between truly experimental information and information which may be introduced from other sources such as model calculations or even guess work. This will not be a severe problem if all input is properly documented. Finally, there is a psychological penalty. Scientists want to have their contributions perceived as clearly identifiable entities. Experimenters like to point to specific cross sections which they have measured. Evaluators take pride in having brought order out of chaos by single-handedly reviewing large bodies of experimental or model calculation results and subsequently producing specific evaluations which they can call their own. The approach discussed in this paper threatens these sensitivities because it implies that the development of nuclear data is more of a team undertaking. Each individual research effort must be viewed as analogous to the contribution provided by a relay runner rather than that by a marathon runner. The possibilities opened by considering this approach seem to this author to be worth these risks. In principle, the nuclear data community should focus on the objective of seeking a better knowledge of nuclear data by whatever legitimate means are available, and relegate matters of individual distinction and achievement to secondary status.

A LEAST-SQUARES METHOD FOR DERIVING REACTION DIFFERENTIAL CROSS SECTION INFORMATION FROM MEASUREMENTS PERFORMED IN DIVERSE NEUTRON FIELDS*

by

Donald L. Smith
Applied Physics Division
Argonne National Laboratory
9700 South Cass Avenue
Argonne, Illinois 60439
USA

ABSTRACT

A generalized least-squares algorithm which refines a prior multi-group energy-differential neutron-reaction cross-section evaluation by addition of new experimental data is described. Complete covariance information for the prior evaluation and for the new experimental information is required in this procedure. The result is a revised best-estimate multi-group cross-section evaluation with complete covariance information. The algorithm tests the consistency of the new and apriori information, and it readily indicates whether the new data significantly improve the knowledge of the differential cross section. These new data need not be specific differential cross sections. Therefore, the experimenter is not limited to measurements which involve only conventional mono-energetic techniques. This opportunity suggests exploration of diverse new experimental methods, e.g., ones which can exploit the high yield and favorable neutron-energy ranges offered by certain unconventional neutron sources which have received little past attention. This method is demonstrated by the detailed analysis of several hypothetical numerical examples. The understanding of the method's potential and limitations which has emerged from the present investigation is discussed.

I. INTRODUCTION

A strong emphasis on nuclear data evaluations during the past several years has led to the dramatic refinement of evaluation techniques, culminating in the development of unbiased generalized least-squares methods and rigorous consideration of covariances for physical quantities (e.g., see Refs. 1-15). This growing sophistication of the evaluation process is forcing experimenters to approach their work in new ways. For example, sharp distinctions between differential and integral methods are fading. Also, experiments are now more likely to be conceived with the evaluation process in mind rather than to provide stand-alone information. This trend is likely to accelerate in the future.

The only reasonable long-term goal for the nuclear data field is the acquisition of fundamental differential information of adequate scope and accuracy to meet all applied needs. Integral results which are inseparable from specific applications may very well have short useful life spans. Expenditure of significant resources to develop such limited data is inadvisable [16]. However, in view of the mathematical tools now available for data analysis, it appears worthwhile to consider very carefully what types of experimental data might be useful in future investigations designed to improve the knowledge of differential parameters. There is a parallel need for creative thinking regarding measurement concepts which would break away from the traditional confines and enable the nuclear data community to achieve significant progress over the next several years.

It is reasonable to question whether the improvement of our knowledge of energy-differential neutron reaction cross sections has to be limited in scope to the restrictive domain of conventional monoenergetic measurement technique. It is well known that valuable cross section normalization information can be derived from careful integral experiments. Can shape information also be derived from certain integral data? There are limited possibilities for tailoring reactor spectra, and the Cf-252 spontaneous-fission neutron spectrum and other radioactive-neutron-source spectra are essentially fixed. Only rudimentary shape information is likely to be inferred from measurements in these neutron fields. On the other hand, diverse integral neutron-spectrum shapes can be generated by bombarding various targets with variable-energy light-charged-particle beams produced by accelerators. The possibility of deriving useful shape information from measurements in these fields seems worthy of investigation. The present state of knowledge of neutron sources used for neutron data development is reasonably well summarized by the papers in Ref. 17. One is impressed by the considerable variety of available neutron sources. It is also evident that severe (and probably unnecessary) restrictions have been placed upon utilization of these neutron sources because of the preconceived notion that useful measurements must generally employ either nearly-monoenergetic sources or sources with spectra which closely resemble those encountered in specific applications.

When measurements can be performed under nearly monoenergetic conditions, the relationship between what is actually measured and a differential cross section is relatively direct [18]. Information provided by broad-spectrum measurements is more subtle in nature and cannot be related directly to the

differential cross sections at any specific energy. Spectrum-average cross
sections depend intimately upon the neutron spectra in question. No fundamental
cross section information can be extracted without detailed quantitative
knowledge of these spectra. It is reasonable, therefore, to question whether
matters should be further complicated by considering the possibility of
performing measurements in various as-yet-not-very-well characterized integral
neutron spectra. The answer to this question emerges when one examines the
properties of those essentially-monoenergetic neutron sources provided by
Nature (e.g., Refs. 16 and 17). The consequences of very serious limitations
in the intensities and useful energy ranges for these sources are readily
apparent in compilations of experimental neutron differential cross sections
(e.g., Ref. 19). As an example, consider the obvious paucity of reliable
cross section data for the neutron-energy range from ~10 MeV to just below 14
MeV. This situation exists because there is no convenient monoenergetic
neutron source reaction which covers this energy range. The quality of cross
section information for reactions with very small cross sections, or for those
where limited availability of material dictates small research samples, is
generally poor owing to the limited intensity of many monoenergetic sources
(e.g., Ref. 16, 17 and 19).

Figure 1 indicates, as an example, the neutron-energy-range coverage
which could be achieved at the Argonne National Laboratory FNG accelerator
facility [20] by means of proton and deuteron bombardment of several promising
target materials [21]. The neutron energy range 0-22 MeV is completely
covered by incident proton and deuteron beams from 2-7 MeV. A rich variety of
quasi-monoenergetic, multiple-discrete-group and continuum-neutron spectra can
be produced by varying the accelerator energy, target compositions and target
thicknesses. Neutron production can be very copious for some of these reac-
tions. For example, 7-MeV deuteron bombardment of a beryllium metal target
which is thick enough to stop the incident deuterons produces a neutron yield
near zero degrees of $\sim 5 \times 10^9$ neutrons/(μCsr) [22]. Furthermore, these are
near-point sources and accelerators may be pulsed so that the spectra can,
in principle, be characterized by means of time-of-flight measurements.

A mathematical procedure which can be used to derive differential cross
section information from the measurements described in the preceding paragraphs
of this section has already been proposed by Perey, but in a different context
[2,4]. Perey has very carefully examined the important reactor dosimetry
problem which involves estimation of the shape and intensity of reactor spectra
by means of an examination of integral reaction rate data and differential
reaction cross section information (e.g., Ref. 23). What is proposed here is
to apply the same mathematical formalism to what is essentially the inverse
problem, namely the estimation of a specific reaction differential cross
section by examination of integral reaction data and information on various
neutron spectra used in the measurements.

The mathematical formalism has been fully described by Perey [2,4], so
certain details and formula derivations will be omitted in the discussion
which follows in Section II. However, the description of the method in
Section II is sufficiently self-contained to enable the reader to follow all
essential steps in the development of this method, as it relates to the
present application, without having to refer constantly to Perey's papers.
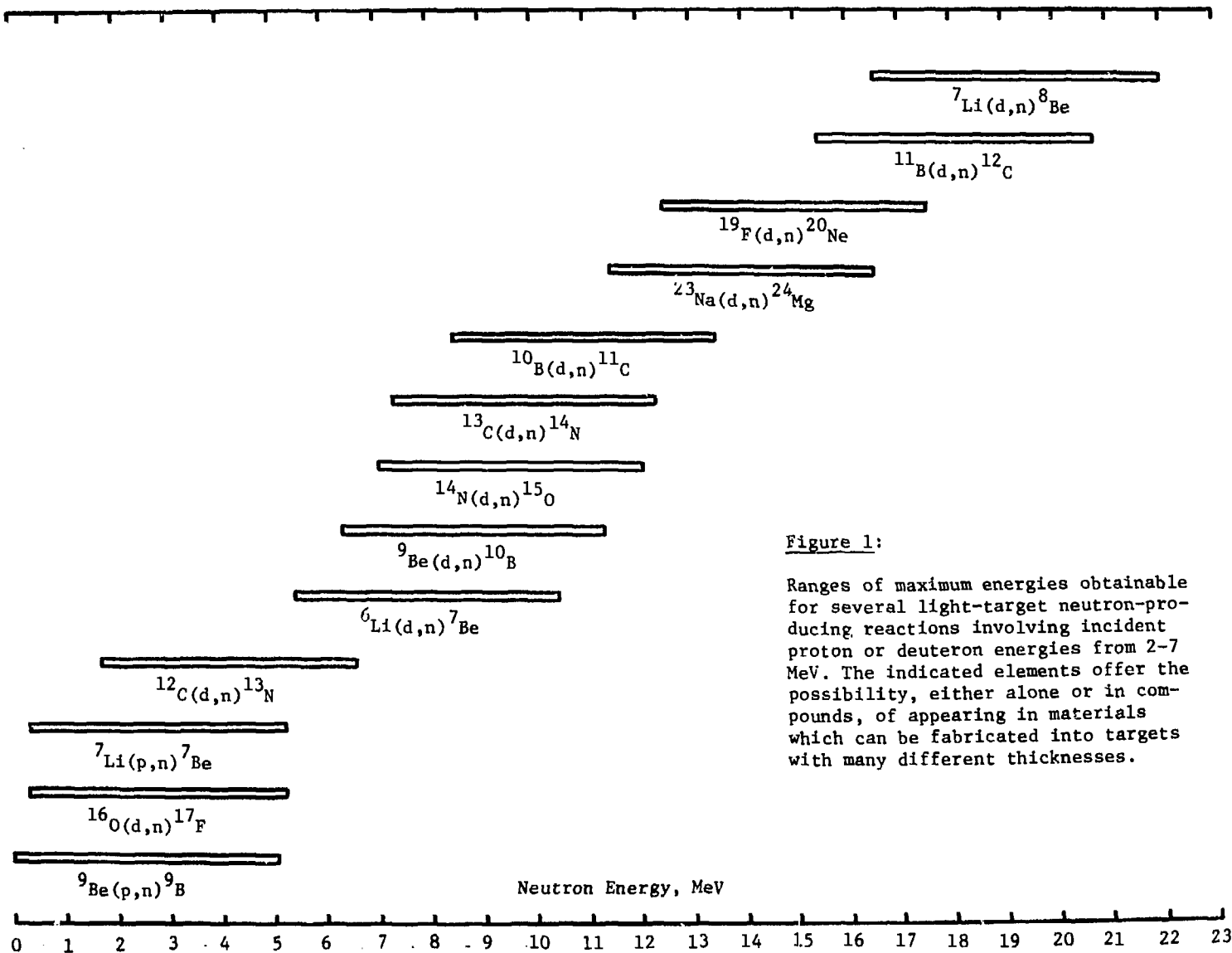
Figure 1:

Ranges of maximum energies obtainable for several light-target neutron-producing reactions involving incident proton or deuteron energies from 2-7 MeV. The indicated elements offer the possibility, either alone or in compounds, of appearing in materials which can be fabricated into targets with many different thicknesses.

^{7}Li(d,n)^{8}Be

^{11}B(d,n)^{12}C

^{19}F(d,n)^{20}Ne

^{23}Na(d,n)^{24}Mg

^{10}B(d,n)^{11}C

^{13}C(d,n)^{14}N

^{14}N(d,n)^{15}O

^{9}Be(d,n)^{10}B

^{6}Li(d,n)^{7}Be

^{12}C(d,n)^{13}N

^{7}Li(p,n)^{7}Be

^{16}O(d,n)^{17}F

^{9}Be(p,n)^{9}B

Neutron Energy, MeV

0   1   2   3   .4   5   6   .7   .8   .9   .10   11   12   13   14   15   16   17   18   19   20   21   22   23

The notation which is used in this paper follows that of Perey to a large extent, thereby facilitating comparison of these two expositions. The reader should be aware, however, that the roles of cross section and spectrum are interchanged, so comparison of specific equations in this work with corresponding ones in the papers of Perey requires attention to this detail.

In order to understand how this method works in practice, it has been applied to several hypothetical numerical examples, constructed so that they test key features of the algorithm. This investigation has been carried out using the program UNFOLD (see Appendix) which has been developed at Argonne National Laboratory specifically for this purpose. The details of this numerical work are reported in Section III. A number of comments on various features of this method appear throughout Sections III and IV.

II. FORMALISM

A neutron differential cross section is never measured directly. Instead, one measures a reaction yield or reaction rate a_q which is related to the differential cross section $\sigma(E)$ by means of a Fredholm integral equation of the first kind [24], expressed as

$$a_q = \int_0^\infty \phi_q(E)\sigma(E)dE. \tag{1}$$

The kernel function ϕ_q is the energy-dependent neutron fluence, suitably normalized to validate Eq. (1). Here, we employ the parameter "q" to identify the specific conditions of the measurement. Clearly, the measured quantity a_q depends intimately upon both $\sigma(E)$ and $\phi_q(E)$.

An idealized monoenergetic experiment to determine a specific cross section value $\sigma(E_q)$ could be performed if the kernel function ϕ_q, hereafter designated as the "spectrum", were of the form

$$\phi_q(E) = \psi_q \delta(E - E_q), \tag{2}$$

with δ defined as the Dirac delta function. The solution to Eq. (1) is trivially

$$\sigma(E_q) = a_q/\psi_q. \tag{3}$$

This idealized measurement would yield the point differential cross section given knowledge of the reaction yield and total neutron intensity.

Realistic experimental measurements involve spectra ϕ_q of finite width localized to an energy range (E_ℓ, E_h). We can write

$$a_q = \int_{E_\ell}^{E_h} \phi_q(E)\sigma(E)dE \tag{4}$$

as a special case of Eq. (1), where ϕ_q vanishes for energies lower than E_ℓ or higher than E_h. If a_q and $\phi_q(E)$ are known, it is possible to relate what is measured to a special cross section in the following fashion: Consider the quantity $\langle\sigma_q\rangle$ given by the formula

$$\langle\sigma_q\rangle = \int_{E_\ell}^{E_h} \phi_q(E)\sigma(E)dE \bigg/\!\!\bigg/ \int_{E_\ell}^{E_h} \phi_q(E)dE. \tag{5}$$

This defines what is commonly referred to as the spectrum-average cross section of $\sigma(E)$ in $\phi_q(E)$. Clearly,

$$a_q = \langle \sigma_q \rangle \int_{E_\ell}^{E_h} \phi_q(E)dE, \tag{6}$$

and, by analogy to Eq. (3), it follows that the spectrum-average cross section can be deduced from a reaction yield measurement and knowledge of the total neutron intensity - without regard to spectrum details.

A knowledge of $\langle \sigma_q \rangle$ generally provides only limited insight into what the point cross section $\sigma(E)$ might be at any specific energy in the range (E_ℓ, E_h). However, if the range (E_ℓ, E_h) is sufficiently narrow so that $\sigma(E)$ varies only a little over this interval, and without sharp fluctuations, we can proceed as follows: Define an average energy E_q for the interval, according to the expression

$$E_q = \int_{E_\ell}^{E_h} \phi_q(E)EdE \Big/\!\!\Big/ \int_{E_\ell}^{E_h} \phi_q(E)dE, \tag{7}$$

and then expand $\sigma(E)$ formally in a Taylor's series about E_q over this interval. Thus,

$$\sigma(E) = \sigma(E_q) + \sigma^1(E_q)(E - E_q) + (1/2)\sigma^2(E_q)(E - E_q)^2 \quad , \tag{8}$$

where $\sigma^i(E_q)$ is the i-th derivative of σ at energy E_q.

This infinite series is truncated at second order under the assumption that higher-order terms are negligible. Substitution of Eq. (8) into Eq. (4) yields the expression

$$a_q = \sigma(E_q) \int_{E_\ell}^{E_h} \phi_q(E)dE + (1/2)\sigma^2(E_q) \int_{E_\ell}^{E_h} \phi_q(E)(E - E_q)^2 dE. \tag{9}$$

The linear term has vanished in Eq. (9) by virtue of the definition of E_q, as state in Eq. (7). Comparison of Eqs. (6) and (9) leads to the expression

$$\sigma(E_q) = \langle \sigma_q \rangle - \left[\frac{\sigma^2(E_q) \int_{E_\ell}^{E_h} \phi_q(E)(E - E_q)^2 dE}{2 \int_{E_\ell}^{E_h} \phi_q(E)dE} \right]. \tag{10}$$

The term in brackets [...] is generally small - if not negligible - for the conditions indicated earlier in this paragraph. Given these nearly-monoenergetic conditions, the spectrum-average cross section is a good approximation to the point cross section $\sigma(E_q)$ [18]. The small indicated correction can be calculated by estimating the second derivative of the differential cross section at E_q.

Next, we proceed to a more complicated situation. Suppose that ϕ_q can be expressed in the form

$$\phi_q(E) \;=\; \sum_{j=1}^{n} \phi_{qj}(E), \tag{11}$$

and that all of the ϕ_{qj} are localized respectively to energy intervals $(E_{\ell j}, E_{hj})$ which do not overlap, as indicated by the conditions

$$\left.\begin{array}{l} E_{h,\,j-1} < E_{\ell,\,j}, \\[2ex] E_{hj} < E_{\ell,\,j+1} \end{array}\right\} \quad (j = 2,\ n-1). \tag{12}$$

Then

$$\int_0^\infty \phi_q(E)dE \;=\; \sum_{j=1}^{n} \int_{E_{\ell j}}^{E_{hj}} \phi_{qj}(E)dE. \tag{13}$$

We thus have a spectrum consisting of n isolated (discrete) groups. Such spectra can be produced by many nuclear reactions, provided that the targets are sufficiently thin to permit the groups to be resolved.

The measured reaction yield a_q is given by

$$a_q \;=\; \sum_{j=1}^{n} \int_{E_{\ell j}}^{E_{hj}} \phi_{qj}(E)\sigma(E)dE \quad, \tag{14}$$

according to Eqs. (4) and (13). If a set of quantities $\langle\sigma_{qj}\rangle$ is defined, analogous to Eq. (5), according to the formula

$$\langle\sigma_{qj}\rangle \;=\; \int_{E_{\ell j}}^{E_{hj}} \phi_{qj}(E)\sigma(E)dE \;\Bigg/\; \int_{E_{\ell j}}^{E_{hj}} \phi_{qj}(E)dE, \tag{15}$$

then

$$a_q \;=\; \sum_{j=1}^{n} \langle\sigma_{qj}\rangle \int_{E_{\ell j}}^{E_{hj}} \phi_{qj}(E)dE, \tag{16}$$

analogous to Eq. (6). The $\langle\sigma_{qj}\rangle$ can be designated as group spectrum-average cross sections. Furthermore, we can define group-average energies E_{qj} by

$$E_{qj} \;=\; \int_{E_{\ell j}}^{E_{hj}} \phi_{qj}(E)EdE \;\Bigg/\; \int_{E_{\ell j}}^{E_{hj}} \phi_{qj}(E)dE, \tag{17}$$

following the form of Eq. (7). If each of the n groups is nearly monoenergetic, then

$$a_q \approx \sum_{j=1}^{n} \sigma(E_{qj}) \int_{E_{\ell j}}^{E_{hj}} \phi_{qj}(E)dE. \tag{18}$$

Small deviations of the point cross sections $\sigma(E_{qj})$ from corresponding group spectrum-average cross sections $\langle \sigma_{qj} \rangle$ can be estimated from formulas similar to Eq. (10).

If there is no dominant term in Eq. (18), we are at an impasse because there is no unique solution for the various $\sigma(E_{qj})$ values, even when a_q and the $\phi_{qj}(E)$ are known. Too much knowledge is demanded from the available information. Suppose, however, that there is one dominant term, designated by "i", and that a prior estimate $\sigma_0(E)$ of the differential cross section is available. Furthermore, let us designate the group flux by ϕ_{qj},

$$\phi_{qj} \equiv \int_{E_{\ell j}}^{E_{hj}} \phi_{qj}(E)dE, \tag{19}$$

and the point cross sections $\sigma(E_{qj})$ and $\sigma_0(E_{qj})$ by σ_{qj} and σ_{oqj}, respectively, to simplify the equations. Then

$$a_q \approx \sigma_{qi}\phi_{qi} + \sum_{j\neq i}^{n} \sigma_{qj}\phi_{qj}, \tag{20}$$

and so

$$\sigma_{qi} \approx (a_q - \sum_{j\neq i}^{n} \sigma_{qj}\phi_{qj})/\phi_{qi}$$

$$\approx a_q \left/ \left[\phi_{qi} + \sum_{j\neq i}^{n} (\sigma_{oqj}/\sigma_{oqi})\phi_{qj} \right] \right. . \tag{21}$$

This approach enables researchers to obtain approximate point cross sections from quasi-monoenergetic results [18]. It must be realized that this method relies on some apriori knowledge of at least the _shape_ of the cross section since _ratios_ of point cross sections for σ_0 appear in Eq. (21). The uncertainty in σ_{qi} must then reflect uncertainties due to the apriori σ_0 , the experimental a_q and ϕ_{qj}, as well as the approximations implicit in Eq. (21).

The preceding development defines the limits of conventional "monoenergetic" measurement technique. In order to apply the preceding formulas, one must select the conditions of an experiment to be in harmony with the various approximations. These limitations and their general impact upon the existing data base were mentioned in Section I.

In order to set the stage for development of a different method for deriving differential cross section information, it is necessary to return to Eq. (4). Let us subdivide the interval (E_ℓ, E_h) into n contiguous-group intervals $(E_{\ell j}, E_{jh})$. They need not be equally wide, but they must span the complete interval (E_ℓ, E_h) and be contiguous according to the conditions

$$
\left.
\begin{aligned}
E_{\ell 1} &= E_\ell, \\
E_{\ell j} &= E_{h, j-1}, \\
E_{hj} &= E_{\ell, j+1}, \\
E_{hn} &= E_h,
\end{aligned}
\right\} \quad (j = 2, n - 1).
\tag{22}
$$

This defines a conventional energy-group structure. We demand of the differential cross section $\sigma(E)$ that it not vary too rapidly over any particular group interval. For example, we might insist that for any interval the function can be reasonably well represented by a second-order Taylor's series expansion about the group median energy E_j defined by

$$
E_j = (1/2) (E_{\ell j} + E_{hj}) \qquad (j = 1, n),
\tag{23}
$$

analogous to the assumptions which led to Eq. (8). Selection of a group structure to utilize in any analysis should be guided by the need to satisfy this requirement. If the differential cross section fluctuates severely with energy, the method under discussion in this paper is in jeopardy unless one is able to work with a very fine group structure (large n).

One readily proceeds from Eq. (4) to the result

$$
a_q = \sum_{j=1}^{n} \langle \sigma_{qj} \rangle \phi_{qj},
\tag{24}
$$

where

$$
\langle \sigma_{qj} \rangle = \int_{E_{\ell j}}^{E_{hj}} \phi_q(E) \sigma(E) dE / \phi_{qj},
\tag{25}
$$

$$
\phi_{qj} \equiv \int_{E_{\ell j}}^{E_{hj}} \phi_q(E) dE.
\tag{26}
$$

On the surface, it would appear that this amounts to a restatement of Eqs. (14)-(16) and (19). However, the imposition of an artificial contiguous-group structure hints that the development now will proceed in a different direction than it did previously.

Let us define a group-average cross section by the formula

$$\langle \sigma_j \rangle = \int_{E_{\ell j}}^{E_{hj}} \sigma(E) dE / (E_{hj} - E_{\ell j}). \tag{27}$$

This quantity differs conceptually from the group spectrum-average cross section $\langle \sigma_{qj} \rangle$ defined by Eq. (25). The group-average cross section does not depend at all on the spectrum $\phi_q(E)$. The difference between the group-average and group spectrum-average cross sections can be estimated from an approximate formula which is derived by expanding $\sigma(E)$ in a second-order Taylor's series around E_j, making use of the definitions of the group spectrum-average energy E_{qj} given by Eq. (17) and the group median energy E_j from Eq. (23). The result is

$$\langle \sigma_j \rangle \approx \langle \sigma_{qj} \rangle - \sigma^1(E_j)(E_{qj} - E_j)$$

$$+ \sigma^2(E_j) \left[(1/24) (E_{hj} - E_{\ell j})^2 + (1/2\phi_{qj}) \int_{E_{\ell j}}^{E_{hj}} \phi_q(E)(E - E_j)^2 dE \right], \tag{28}$$

with ϕ_{qj} interpreted as the group flux according to Eq. (26). In order to evaluate this difference numerically, the first and second derivatives of σ must be estimated at E_j from apriori information.

The point is that when an appropriate group structure is selected, and the stated conditions for $\sigma(E)$ are reasonably-well satisfied, then the difference between $\langle \sigma_j \rangle$ and $\langle \sigma_{qj} \rangle$ will be quite small for all the groups and we can rewrite Eq. (24) as

$$a_q \approx \sum_{j=i}^{n} \langle \sigma_j \rangle \phi_{qj}. \tag{29}$$

Equation (29) relates a measured reaction yield a_q to group fluxes and group cross sections for one measurement performed under a specific set of conditions designated by "q". Now consider a set of m measurements, each involving a distinct condition. Eq. (1) is generalized to the following set of equations

$$a_i = \int_0^\infty \phi_i(E)\sigma(E) dE \qquad (i = 1, m), \tag{30}$$

with the subscript "i" designating a particular measurement much as "q" did in the preceding discussion. For any such set of measurements, there exists a finite energy interval (E_ℓ, E_h) such that $\phi_i(E)\sigma(E)$ vanishes outside the interval for <u>every</u> "i". A group structure can be generated as described by Eq. (22) and the associated paragraph. Furthermore, approximations identical to those described in Eqs. (23) - (29) can be made so that

$$a_i \approx \sum_{j=1}^{n} \phi_{ij}\sigma_j \qquad (i = 1, m), \tag{31}$$

with σ_j equivalent to $\langle\sigma_j\rangle$.

For the special case where m=n, there may be a unique solution to the coupled system of equations represented by Eq. (31). In Section III it is shown that although an experimenter could contrive to perform a sequence of integral measurements equal in number to the group structure mesh, this is not a useful procedure. The flaw can be traced to uncertainty propagation considerations.

From this point on, this development merges with that of Perey [2,4], but the notation is appropriately altered to conform with the present physical problem rather than with the dosimetry problem which he addresses. A definition of the notation is in order:

A set of m measured reaction yields $\{a_{oi}\}$ is designated by the vector A_o. Associated with these measured quantites is the covariance matrix N_{Ao}. The set of m x n group fluxes $\{\phi_{ij}\}$ also represents experimental information. For a fixed "i", the n-fold subset $\{\phi_{ij}\}$ forms a vector designated as Φ_i. The set of m vectors $\{\Phi_i\}$ is designated as Φ. Associated with Φ, now considered as an m x n-dimensional vector, is the covariance matrix $N\Phi$ of dimension [(m x n), (m x n)]. We will also refer to submatrices $N_{\Phi ij}$ of N_{Φ}, each of which has dimension (n,n) with i,j = 1, m in this instance. This algorithm also requires apriori knowledge of the cross section which we represent in group format by the set of values $\{\sigma_j\}$ which form the apriori vector σ. The assumed covariance matrix for σ is $N\sigma$. Also, we will speak of a set of m <u>calculated</u> reaction yields $\{a_i\}$ designated by the vector A. Following Eq. (31), and the notation thus far introduced, we write

$$a_i = \sum_{j=1}^{n} \phi_{ij}\sigma_j = \Phi_i^+ \bullet \sigma \qquad (i = 1, m), \tag{32}$$

where the symbol "+" indicates matrix transposition, and "$\bullet$" symbolizes matrix multiplication.

Equation (32) is the exact mathematical expression of the <u>model</u> which is assumed in the quest for a solution to the present problem. The measured quantities A_O and the quantities A, which are calculated from apriori σ and the experimental group fluxes Φ by means of Eq. (32), are certainly related, but the reader must clearly understand their distinct origins in order to fully comprehend the algorithm which is described below.

Now, consider both σ and Φ as vectors and define another vector P, designated as the parameter vector, according to the expression

$$P = \begin{bmatrix} \sigma \\ \Phi \end{bmatrix}. \tag{33}$$

Associated with P is the covariance matrix N_p. We make the important assumption that no correlations exist between uncertainties for the assumed apriori group cross sections σ and the group fluxes Φ. Then

$$N_p = \begin{bmatrix} N_\sigma & 0 \\ 0 & N_\Phi \end{bmatrix}, \tag{34}$$

with the zeros representing zero matrices of appropriate dimensionality.

A comment about the assumption which leads to Eq. (34) is in order at this point. The neutron spectrum from Cf-252 spontaneous fission and accelerator-produced spectra can be measured by the conceptually-simple time-of-flight technique. Thus, they can generally be expected to satisfy the condition indicated in Eq. (34). The situation for reactor spectra is not so obvious. Determination of these spectra generally involves recourse to considerable nuclear cross section information. Reactor calculations require scattering and reaction cross section data. Reactor dosimetry methods involving reaction rate measurements and spectrum unfolding are also heavily dependent upon cross section data [4,23]. So, for reactor neutron spectra it is very possible that there are implicit correlations between σ and Φ which would be difficult to trace, but which invalidate Eq. (34). This possibility must be considered before attempting to utilize reactor-spectrum integral results in an analysis of the type proposed in this paper.

Perey discusses the philosophical and mathematical basis of the generalized least-squares method, as applied to the solution of problems such as the one posed by Eq. (31) [2,4,5], and similar expositions appear in other references (e.g., Refs. 1, 3, 6, 8, 10-14). Many of these details will be omitted in the following discussion to avoid redundancy.

Suppose Y represents a complete set of input parameters for a problem and N_Y is its covariance matrix. The generalized least-squares method involves consideration of the formula

$$\chi^2 = (Y - \hat{Y})^+ \bullet N_Y^{-1} \bullet (Y - \hat{Y}). \tag{35}$$

Here, "-1" designates inversion of a matrix. Briefly, one seeks to find a revised set of the same parameters, labelled $\hat{Y}$, which <u>minimizes</u> χ^2. Once such a $\hat{Y}$ is found, it is designated to be the solution to the problem and is then labelled Y'. In the present application, Y and $\hat{Y}$ are defined by

$$Y = \begin{bmatrix} P \\ A_o \end{bmatrix},$$

$$\hat{Y} = \begin{bmatrix} \hat{P} \\ \hat{A} \end{bmatrix}, \tag{36}$$

with $\hat{P}$ defined in terms of $\hat{\sigma}$ and $\hat{\phi}$ as in Eq. (33), and $\hat{A}$ consisting of calculated elements $\hat{a}_i$ which are related to $\hat{\sigma}$ and $\hat{\phi}$ according to Eq. (32). The functional relationship

$$\hat{A} = \hat{A}(\hat{P}) \tag{37}$$

implied by Eq. (32) is <u>nonlinear</u>.

A linear approximation to Eq. (37) is needed in order to solve the problem. Perey describes this procedure and its implications at great length in Ref. 4. Based on the model which is represented by Eq. (32), it can be shown that to first order

$$\hat{A} = A + G \bullet (\hat{P} - P), \tag{38}$$

where the relationship between P and A is identical to that between $\hat{P}$ and $\hat{A}$, and G is the matrix

$$G = \begin{bmatrix} \phi_1^+ & \sigma^+ & 0 & \cdots & 0 \\ \phi_2^+ & 0 & \sigma^+ & \cdots & 0 \\ \vdots & & & & \\ \phi_m^+ & 0 & \cdots\cdots & & \sigma^+ \end{bmatrix}. \tag{39}$$

The content of Eqs. (35) – (39) leads to a restatement of the least-squares problem in the linear form

$$\chi^2 = \begin{bmatrix} P - \hat{P} \\ A_o - A - G \bullet (P - \hat{P}) \end{bmatrix}^+ \bullet \begin{bmatrix} N_P & 0 \\ 0 & N_{Ao} \end{bmatrix}^{-1} \bullet \begin{bmatrix} P - \hat{P} \\ A_o - A - G \bullet (P - \hat{P}) \end{bmatrix}, \tag{40}$$

provided that it is assumed that the uncertainties for the parameters P are uncorrelated to those for A_o so that

$$N_Y = \begin{bmatrix} N_P & 0 \\ 0 & N_{Ao} \end{bmatrix}. \tag{41}$$

Determination of the best solution P' (the one that minimizes χ^2) is straight-forward but involves tedious matrix algebra. The result according to Perey [4] is

$$P' = P + N_P \bullet G^+ \bullet (N_A + N_{Ao})^{-1} \bullet (A_o - A), \tag{42}$$

and the covariance matrix for this solution is

$$N_P' = N_P - N_P \bullet G^+ \bullet (N_A + N_{Ao})^{-1} \bullet G \bullet N_P^+, \tag{43}$$

with

$$N_A = G \bullet N_P \bullet G^+. \tag{44}$$

There are several comments to be made concerning this solution. Since the original minimization problem has been linearized, the solution will be reliable only if P' does not differ too violently from the initial conditions P. Furthermore, the search for a minimum must take place in the vicinity of the true minimum and not near a local "false" minimum. These conditions are characteristic of all non-linear problems. Also, it is clear that this algorithm formally adjusts the group fluxes as well as the group cross section values, according to Eq. (33). This point may very well trouble the reader since it can be argued that the group fluxes are experimentally measured, just as are the reaction yields, and therefore they should not be adjusted in a problem where the quest is for revised group cross sections only. Again, Perey had discussed this point in detail [4]. The reader may find this unavoidable feature of the least-squares method more palatable if he realizes that the input quantities A_o, Φ and σ all have uncertainties, and that the problem as posed by Eq. (31) usually has no unique solution but only a best, or most-probable, solution in the least-squares sense. Detailed inspection of Eqs. (42) and (43) indicates that evaluation of the solution involves only the inversion of an (m,m) matrix rather than inversion of a much larger matrix as one might have expected from Eq. (40). Finally, it is important to repeat the advise of Perey, who states that it is generally inadvisable to iterate the problem in order to achieve a better solution. Of course, one can formally iterate, but interpretation of the solution then becomes uncertain [4].

Perey has shown that the minimum χ^2, corresponding to the solution P', is given by the relatively-simple expression

$$\chi_m^2 = (A_o - A)^+ \bullet (N_A + N_{Ao})^{-1} \bullet (A_o - A). \tag{45}$$

It is evident from this particular formula that χ_m^2 depends only upon the input information [4]. Therefore, it can be calculated before the least-squares minimization is performed, and the result then utilized to test the consistency of all the input information. Perey discusses various aspects of the consistency-testing process [2,4]. Here we simply mention that the quantity (χ_m^2/m), which is the chi-square per degree of freedom, should be in the range 0.3-2. Values outside this range are very unlikely and indicate inconsistencies in the input information [2].

Equations (42)-(45) are not very useful for numerical work, so we now present some formulas which can be readily programmed on a computer to yield the quantities we would like to have for the solution. First, we realize that Eqs. (42)-(44) provide much more than we actually want. We will be satisfied to have expressions for elements $\{\sigma_j'\}$ of the revised groups cross section σ',

and its covariance matrix N'_σ. The quantity χ^2_m certainly should be calculated in order to test the consistency of the input information.

We avoid burdening the reader with tedious detail and simply list the formulas needed to calculate the desired solution. Let us define c_{ij} by

$$a_i = \sum_{j=1}^{n} c_{ij} \qquad (i = 1,m),$$

$$c_{ij} = \phi_{ij}\sigma_j \qquad (i = 1,m; \; j = 1,n). \tag{46}$$

N_A as defined by Eq. (44) can be expressed as the sum of two matrices according to

$$N_A = N_A^\sigma + N_A^\phi, \tag{47}$$

where

$$(N_A^\sigma)_{ij} = \phi_i^+ \bullet N_\sigma \bullet \phi_j = \sum_{k=1}^{n} \sum_{\ell=1}^{n} \phi_{ik}(N_\sigma)_{k\ell}\phi_{j\ell} \qquad (i,j = 1,m), \tag{48}$$

$$(N_A^\phi)_{ij} = \sigma^+ \bullet N_{\phi ij} \bullet \sigma = \sum_{k=1}^{n} \sum_{\ell=1}^{n} \sigma_k(N_{\phi ij})_{k\ell}\sigma_\ell \qquad (i,j = 1,m). \tag{49}$$

Thus, the matrix V defined by

$$V = N_{Ao} + N_A^\sigma + N_A^\phi, \tag{50}$$

can be calculated readily and then inverted to give the matrix W. Now, define elements u_{ij} by

$$u_{ij} = \sum_{k=1}^{n} (N_\sigma)_{jk} c_{ik}/(\sigma_j\sigma_k) \qquad (i=1,m; j=1,n). \tag{51}$$

Then the solution σ' and covariance matrix N'_σ can be calculated using the formulas

$$\sigma'_j = \sigma_j \left[1 + \sum_{k=1}^{m} \sum_{\ell=1}^{m} u_{kj}w_{k\ell}(a_{o\ell} - a_\ell) \right] \qquad (j = 1,n), \tag{52}$$

$$(N'_\sigma)_{ij} = (N_\sigma)_{ij} - \sigma_i\sigma_j \sum_{k=1}^{m} \sum_{\ell=1}^{m} w_{k\ell}u_{ki}u_{\ell j} \qquad (i,j = 1,n). \tag{53}$$

Furthermore,

$$\chi_m^2 = \sum_{k=1}^{m} \sum_{\ell=1}^{m} (a_{ok} - a_k) w_{k\ell} (a_{o\ell} - a_\ell). \tag{54}$$

In Eqs. (48)-(54), the notation $(Z)_{ij}$ is used to designate the i,j-th element of the matrix Z.

This completes the development of the mathematical formalism needed to treat the problem at hand. However, it is instructive to examine the task of specifying Φ and N_Φ for a special case. Suppose that an experimenter decides to generate a family of group fluxes Φ by some technique and to perform an experiment designed to characterize these spectra. To do this would require use of a calibrated detector with a measured efficiency curve $\varepsilon(E)$. The effective efficiency for each group could be represented by the vector ε of elements $\{\varepsilon_j\}$. The measured yield of events for each group could be labelled ν_{ij}, quantities which we assume are subject only to random errors equal to $(\nu_{ij})^{1/2}$. Then

$$\phi_{ij} = \nu_{ij}/\varepsilon_j \qquad (i = 1,m; \; j = 1,n). \tag{55}$$

Elements of the submatrices $N_{\Phi ij}$ of N_Φ can then be expressed in the form

$$\begin{aligned}
(N_{\Phi ij})_{k\ell} &= \delta_{ij}\delta_{k\ell}\phi_{ik}\phi_{j\ell}f_{\nu ik}f_{\nu j\ell} \\
&\quad + \phi_{ik}\phi_{j\ell}(C_\varepsilon)_{k\ell}f_{\varepsilon k}f_{\varepsilon \ell} \\
&\quad + (C_E)_{k\ell}\eta_{Eik}\eta_{Ej\ell}\Delta E_k \Delta E_\ell.
\end{aligned} \tag{56}$$

Here, $f_{\nu ik}$ is the fractional uncertainty in ϕ_{ik} due to random count errors and it is given by

$$f_{\nu ik} = (\nu_{ik})^{-1/2}. \tag{57}$$

The quantity $f_{\varepsilon k}$ is the fractional error involved in measuring flux for the kth group due to detector efficiency uncertainty. C_ε is the efficiency uncertainty correlation matrix [11]. The third term indicates the implicit group-flux uncertainty introduced by uncertainty of the neutron energy scale which is established in the group-flux characterization experiment. The matrix C_E is the group energy-scale uncertainty correlation matrix, ΔE_k is the energy scale uncertainty for the kth group, and η_{Eik} is the sensitivity of ϕ_{ik} to ΔE_k. This development is not completely general, but it demonstrates to the reader how one goes about generating the matrix N_Φ from information of lower rank for a specific class of spectrum measurements. This approach is the one used for the examples presented in Section III.

III. NUMERICAL EXAMPLES

An understanding of the method described in Section II can be acquired in less time, at a lower cost, by employing computer simulation rather than actual experimentation. Therefore, this approach is pursued in the present investigation. For convenience and speed, a rather coarse group structure (n=15) is utilized. In order to avoid serious problems with such a coarse structure, we examine an energy-smooth high-threshold process, namely one with an energy-differential cross section shape characteristic of certain neutron-induced charge-particle production reactions [19]. The fifteen groups are all 0.5 MeV wide and span the energy range 9.5-17 MeV.

Various quasi-realistic families of neutron spectra are considered. These spectra are generated pointwise by linear interpolation of tables for the essentially-continuous neutron spectra. Other spectra are represented pointwise as superpositions of one or more Gaussians which are characterized by the usual parameters. However, these pointwise specifications merely provide the means for calculation of specific fifteen-group representations which are actually utilized in the analyses. A fifteen-group representation of the single cross section curve used in these studies is also generated for comparison with the unfolded results. Owing to the fact that this hypothetical cross section is also represented pointwise by straight-line segments over intervals corresponding to the group structure, the group cross section equals the corresponding point cross section value at the group median energy for each of the fifteen groups.

In order to better simulate reality, for several of the examples in this section those quantities which would correspond to measured quantities in an actual experiment are allowed to vary in order to see how this influences the outcome. In all instances, reaction yields A_0, as defined by Eq. (30), are calculated by precise integration rather than by using the group formula, Eq. (31). The reason is that this is what actually happens in real measurements. Since the group structure is coarse, there are discrepancies which can be directly attributed to the group approximation assumption. For this reason, it is suggested that the reader pay more attention to the qualitative conclusions which can be drawn from the examples presented here than to the specific numerical details. It is the objective of this investigation to examine certain characteristic features of the basic method without becoming distracted by the rather well-understood problems associated with group representation of pointwise-continuous physical quantities.

The differential cross section unfolding calculations, based upon the least-squares algorithm described in Section II, have been performed using the program UNFOLD which is described in the Appendix. No details of the calculation of certain integral-response and group quantities from pointwise functional representations are described since they are very straightforward.

Example 1

Consider the family of hypothetical neutron spectra shown in Fig. 2. Assume that these are produced at an accelerator by bombarding a thick target
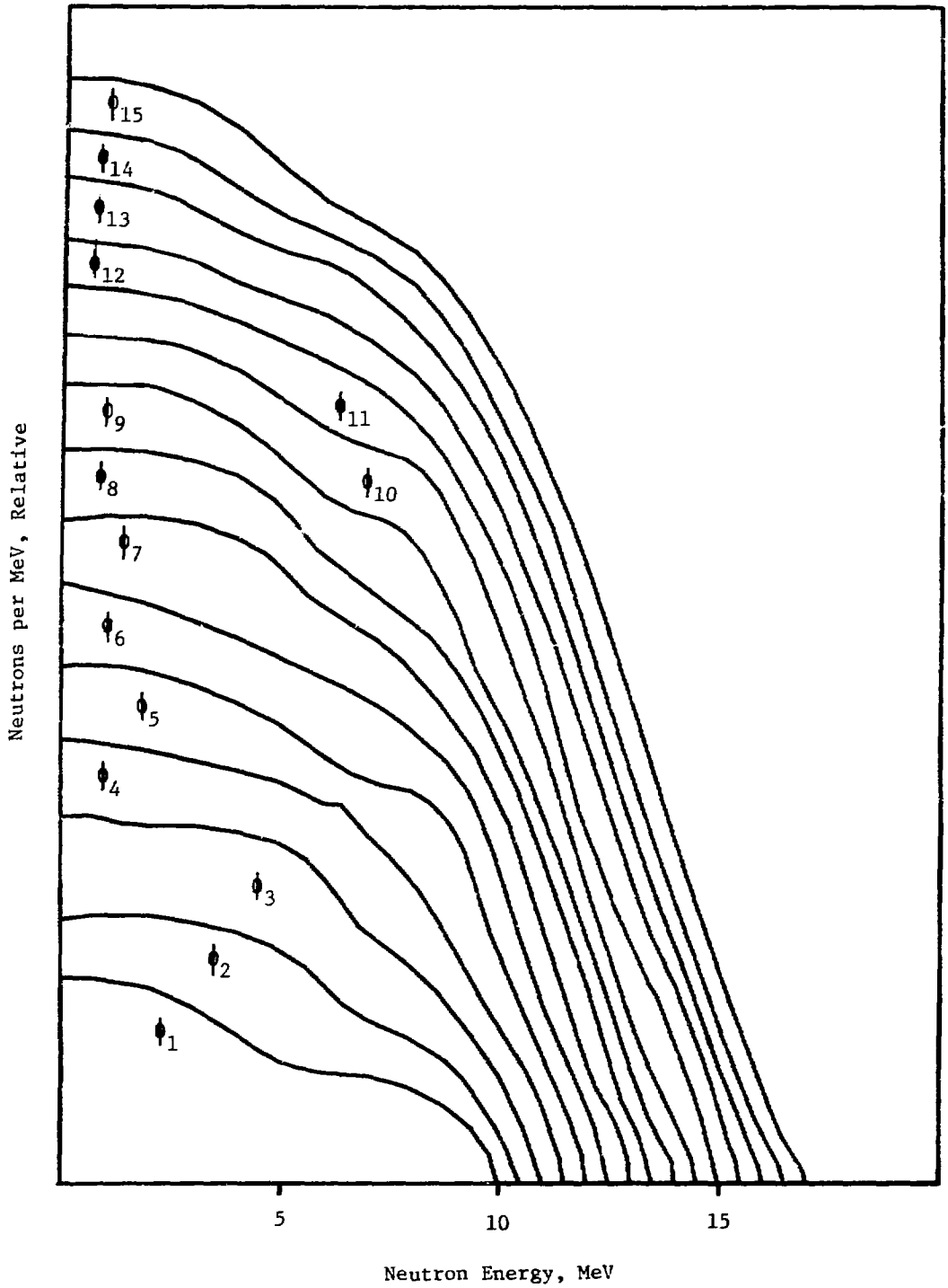
Figure 2: A family of fifteen hypothetical continuous-neutron spectra utilized in simulated cross section unfolding calculations.

at fifteen different charged particle energies. Furthermore, assume that the spectra have been characterized in a separate experiment. Group fluxes for the standard fifteen-group representation (225 in number)are calculated. A group-flux covariance matrix is generated as described in the paragraph of Section II which includes Eqs. (55)-(57). For this example, the random statistical uncertainties derived according to Eq. (57) are all smaller than 3%. The uncertainties due to detector efficiency are all assumed to be 3%, with 50% correlation between any two different groups. The uncertainties resulting from energy scale problems are all smaller than 10% (generally much smaller) resulting from 100% - correlated group-energy uncertainties assumed to be in the range 16-28 keV. The actual simulated energy-differential cross section for this problem appears in Fig. 3.A. The response curves calculated using this cross section, and the family of spectra in Fig. 2, appear in Fig. 3.B. Simulated reaction yields A_0, corresponding to the areas under the curves of Fig. 3.B as calculated using Eq. (30), are presented in Table 1.

Assume for this first example that the experimental group fluxes are precisely as calculated and that the measured reaction yields A_0 are as given in Table 1. Each a_{oi} is assumed to carry an experimental error of 2.8% which is 50% correlated to all other members of the set. Since this example involves fifteen simulated measurements and fifteen unknowns, it is possible in this instance to solve the problem posed by Eq. (31) exactly for the unknown group cross sectons. Also, since this problem is a simulation, the group cross sections can be calculated separately, using the numerical representation of the σ indicated in Fig. 3.A, and Eq. (27). The results are compared in Table 2. The indicated differences in this case are actually the errors introduced by the coarse-group approximation. The errors are of concern for the lowest three groups, but they can be ignored for the remaining groups.

The results obtained by directly solving the problem posed by Eq. (31) are subject to uncertainty because in reality the group fluxes Φ and reaction yields A_0 represent uncertain experimental quantities as indicated above. The effects of these uncertainties can be calculated using standard sensitivity techniques for error propagation [11]. The analysis involves tedious numerical work which is best done using a digital computer. The details are omitted here, but the final results appear in Table 2. The uncertainies are modest for the first few groups; they are actually smaller than the group-approximation error for the first two groups. However, the uncertainties become prohibitively large at higher energies. It is concluded that if the group fluxes and reaction yields could be <u>precisely</u> specified, as they indeed are in this simulation, then one could directly calculate the group differential cross sections. However, when realistic uncertainties are considered for the quantities which would actually be physically measured, then the uncertainties for the derived cross sections become excessively large, except for the first few groups. In short, this approach fails to be useful.

It would seem, then, that the hypothetical integral experiment represented in Figs. 2 and 3 does not offer a very good means for acquiring information about the differential cross section considered in this example. The reason is physically apparent upon reflection. Integral measurements involving the first few spectra (say ϕ_1 through ϕ_4) yield response profiles which are reasonably well-localized in energy (Fig. 3.B). Therefore, one has the opportunity
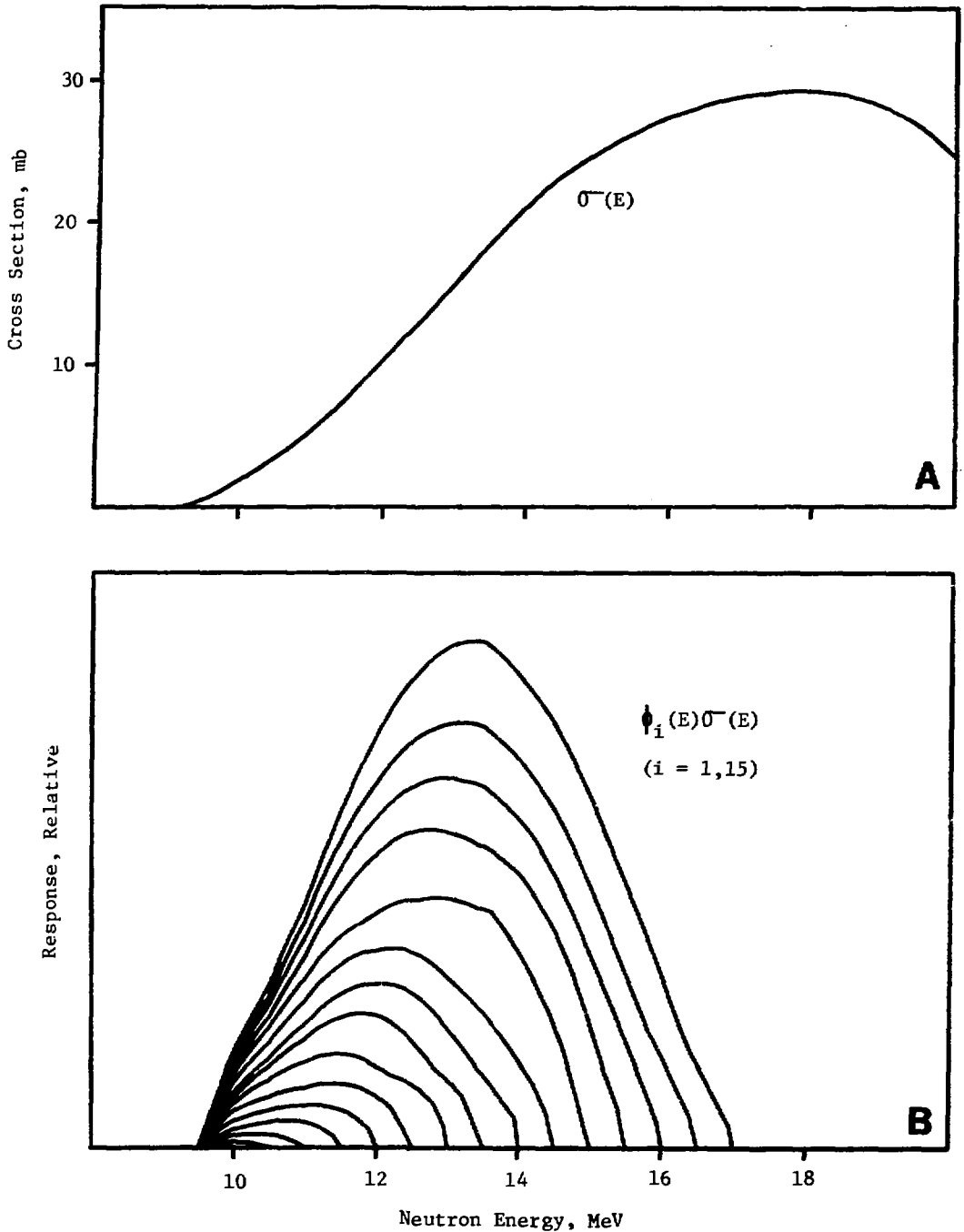
Figure 3: (A) Hypothetical energy-dependent differential cross section used in simulation calculations. (B) A family of fifteen response curves generated from the product of this differential cross section and the spectra in Fig. 2. The response for i=1 is quite narrow and weak (barely visible) while that for i=15 is broad and dominant.

Table 1. Simulated Reaction Yields for Example 1

Spectrum[a] Index	a_{oi}[b]	Spectrum[a] Index	a_{oi}[b]
1	886.95	9	659770.0
2	5464.9	10	903140.0
3	20068.0	11	1299900.0
4	53296.0	12	1740800.0
5	108720.0	13	2121400.0
6	191210.0	14	2536200.0
7	314830.0	15	3124500.0
8	479360.0		

[a]Identifies specific ϕ_i from Fig. 2.

[b]Derived from spectrum ϕ_i and σ given in Fig. 3.A. These values correspond to areas under the curves plotted in Fig. 3.B.

Table 2. Direct Solution Results for Example 1

Group	Actual σ	Difference	Solution σ	
1	0.9	−26.4%	0.66255	(7.2%)
2	2.5	+ 7.7%	2.6915	(7.3%)
3	4.15	− 5.3%	3.9313	(11.9%)
4	6.35	+ 1.9%	6.4697	(16.0%)
5	8.9	− 1.3%	8.7864	(21.0%)
6	11.6	+ 0.1%	11.616	(30.3%)
7	14.4	+ 0.3%	14.447	(37.0%)
8	17.25	− 0.7%	17.130	(56.1%)
9	19.85	+ 1.1%	20.075	(83.3%)
10	22.1	− 0.6%	21.958	(109%)
11	24.05	+ 0.5%	24.174	(154%)
12	25.45	+ 0.1%	25.486	(222%)
13	26.55	− 0.1%	26.527	(287%)
14	27.525	+ 0.1%	27.560	(354%)
15	28.375	Negligible	28.386	(468%)

to derive differential cross section information directly from the data. Put another way, these measurements "resemble" monoenergetic or specifically-differential measurements. The higher-energy groups only become involved for spectra which are quite broad and therefore incapable of yielding much information about differential cross sections for the individual groups. This is not to say that this hypothetical experiment is not useful, but simply that we are demanding too much from it when the data are analyzed by the direct method. Consider, for example, a case where the <u>shape</u> of the hypothetical $\sigma(E)$ is well known. Then it is clear that a good <u>integral</u> measurement with any <u>one</u> of the fifteen spectra shown in Fig. 2 would provide very valuable information capable of defining the cross-section normalization. Clearly what is required is a formalism which enables us to derive useful information from measurements designed to <u>supplement</u> or <u>refine</u> existing knowledge of the cross section. The least-squares formalism described in Section II meets this requirement.

So, next we approach this same problem by another method. In order to do this it is necessary to have an apriori group cross section set with a covariance matrix. In this simulated problem, we will assume the apriori cross section given in Table 3 and Fig. 4. The assumed uncertainties for this apriori are in the range 25-40% and are taken to be uncorrelated in order to avoid introducing any other preconceived information about the cross section. We see that the shape of this apriori cross secton is not quite right, especially near threshold. These conditions, assumed for the purposes of this simulation, are quite typical of what nuclear data researchers encounter in reality. Application of the least-squares algorithm then yields results which are also given in Table 3 and Fig. 4.

The solution is clearly an improvement over the prior knowledge of the cross section. The new data lead to an adjustment of the apriori cross section toward the actual group cross section in <u>all</u> fifteen groups. The influence is most pronounced below ~15 MeV. Above this, the new data are not very influential so the solution trends closer to the apriori than it does to the actual physical group cross section. The solution is really better than it seems from Table 3. The difference between the least-squares solution and the actual group cross section for the lowest two or three groups can be largely attributed to the failure of the coarse-group approximation and not to our unfolding method. Clearly the least-squares method is superior to the direct solution method for this example. It does not demand more from what amounts to the measured information in this simulation than it is able to yield in the way of derived results. Rather than insisting that the measured data yield a full set of cross sections, it provides a framework wherein the data can supplement our existing knowledge of the cross section and thereby guide us toward a better knowledge of it. As seen from Table 3 and Fig. 4, this hypothetical experiment has indeed contributed respectably toward this goal. the revised group cross sections are truly closer to the actual cross section curve (and the derived errors are smaller) than was the case for the apriori, at least below ~15 MeV. This amounts to quantitative proof that the new information is useful. This new solution is, of course, consistent with the outcome of the direct data-evaluation method, as given in Table 2. However, the least-squares algorithm gives us a much better perspective of the whole situation, before and after the hypothetical experiment, for this particular

Table 3. Least-Squares Results for Example 1

Group	Apriori σ	Difference	Actual σ	Difference	Solution σ
1	2 (40%)	+122%	0.9	−21.4%	0.707 (18.4%)
2	3 (33.3%)	+20%	2.5	+6.6%	2.666 (8.2%)
3	5 (30%)	+20.5%	4.15	−2.5%	4.046 (12.9%)
4	9 (33.3%)	+41.7%	6.35	Negligible	6.353 (15.6%)
5	12 (25%)	+34.8%	8.9	+2.2%	9.099 (16.2%)
6	14 (28.5%)	+20.7%	11.6	+1.1%	11.729 (19.3%)
7	14 (28.5%)	−2.8%	14.4	−2.3%	14.067 (20.1%)
8	16 (31.3%)	−7.2%	17.25	−1%	17.806 (20.5%)
9	17 (29.4%)	−14.4%	19.85	−0.6%	19.730 (20.6%)
10	19 (28.9%)	−14.0%	22.1	+3.3%	22.830 (19.7%)
11	20 (25%)	−16.8%	24.05	−3.3%	23.240 (19%)
12	21 (28.6%)	−17.5%	25.45	−2.1%	24.911 (21.2%)
13	20 (30%)	−24.7%	26.55	−14.8%	22.629 (24.8%)
14	22 (31.8%)	−20.1%	27.525	−13.7%	23.750 (28.6%)
15	23 (30.4%)	−18.9%	28.375	−17.1%	23.525 (29.6%)

Solution uncertainty correlation matrix

	1	2	3	4	5	6	7	8	9	10	11	12	13	14	15
1	1														
2	−0.12	1					(symmetric)								
3	0.34	−0.48	1												
4	0.18	0.34	−0.54	1											
5	0.11	−0.01	0.28	−0.53	1										
6	0.07	0.07	0.03	0.14	−0.53	1									
7	0.04	0.05	0.03	0.04	0.09	−0.53	1								
8	0.06	0.06	0.04	0.05	0.07	−0.07	−0.37	1							
9	0.05	0.05	0.03	0.03	0.04	0.07	−0.09	−0.42	1						
10	0.05	0.05	0.03	0.03	0.03	0.07	0.02	−0.16	−0.36	1					
11	0.04	0.04	0.03	0.03	0.02	0.04	0.03	−0.02	−0.12	−0.27	1				
12	0.03	0.04	0.02	0.03	0.02	0.02	0.02	0.01	−0.03	−0.14	−0.23	1			
13	0.02	0.02	0.01	0.02	0.01	0.01	0.01	0.01	0	−0.05	−0.10	−0.18	1		
14	0.01	0.01	0.01	0.01	0.01	0.01	0.01	0.01	0	−0.01	−0.04	−0.09	−0.09	1	
15	0	0	0	0	0	0	0	0	0	0	−0.01	−0.02	−0.02	−0.02	1

$(\chi_m^2/m) = 0.53$

Cross sections: Smooth $\sim$ Apriori group ••• Solution group ——
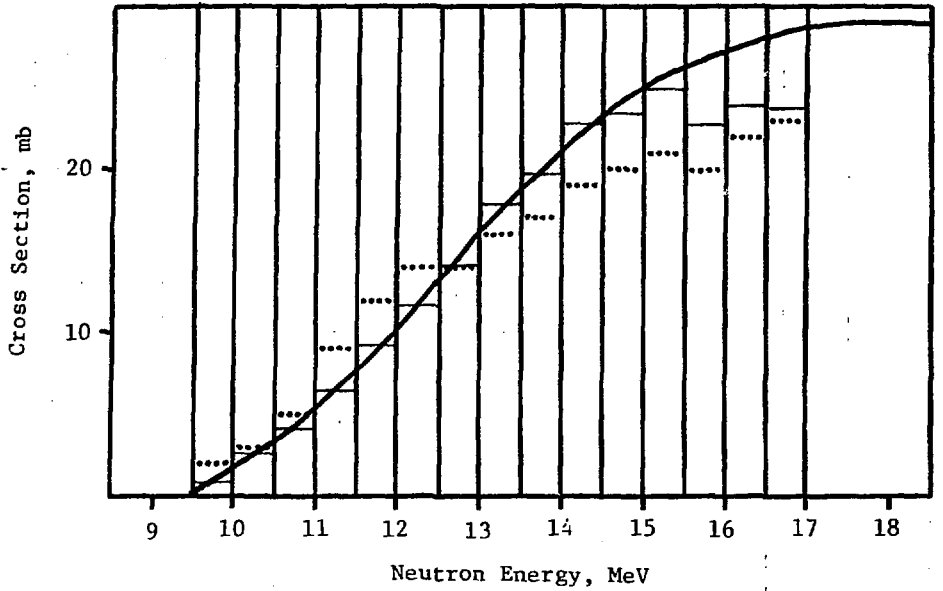

Figure 4: Cross sections for Example 1.

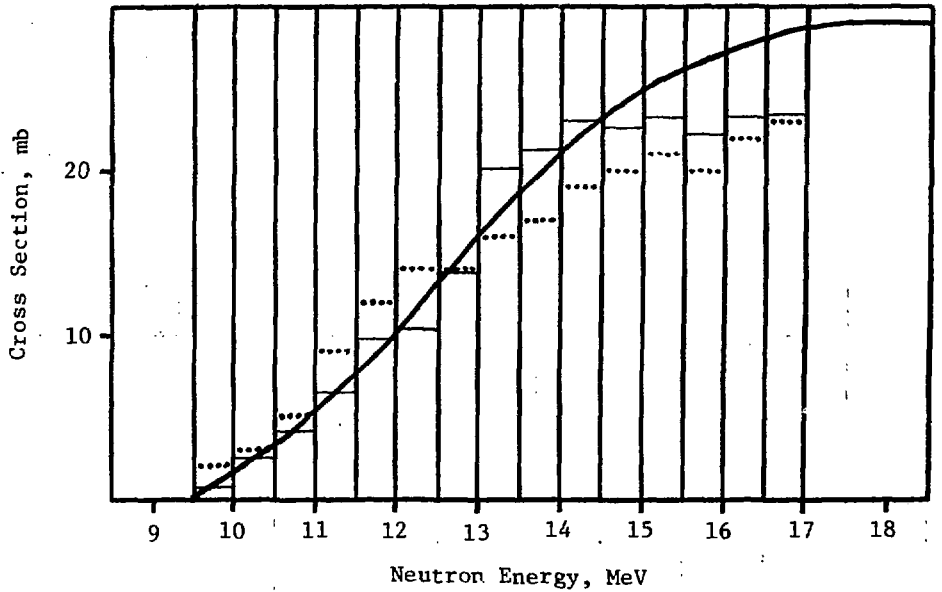Cross sections: Smooth $\sim$ Apriori group ••• Solution group ——

Figure 5: Cross sections for Example 3.

reaction. This demonstrates a fundamental theme of this report, namely that useful differential cross section information <u>can</u> be obtained from various integral measurements. Furthermore, the algorithm produces a solution covariance matrix which, for this example, appears in Table 3 in its entirety. *Remembering that the uncertainties for the apriori cross section were com-*pletely uncorrelated, it is interesting to observe the significant short-range anti-correlation pattern which is a dominant feature of the covariance matrix generated by least-squares analysis of this example.

There is still an important element of reality missing from Example 1. We have utilized for Φ and A_0 the <u>precise</u> values which they would have for the actual $\sigma(E)$ and $\phi_j(E)$ involved in the simulation. To further examine the viability of the method, it is necessary to consider what happens when elements of Φ and A_0 deviate from their true values because of experimental uncertainties. The next several examples will involve simulation of these effects.

Example 2

The effects of variation in the elements of Φ and A_0 can be investigated readily by introducing input data sets which have been prepared by randomly altering selected parameters from their true values, within uncertainties. This task can be accomplished via the Monte-Carlo method quite readily <u>if</u> we relax all correlation assumptions for the parameter uncertainties. Therefore, we will first examine the effect of eliminating these correlations before proceeding with simulations involving variation of Φ and A_0. All input for the present example is thus identical to Example 1 except that the uncertainty *correlations are deleted. Results of a least-squares analysis of this problem* appear in Table 4. For economy we omit the solution covariance matrix from this and all further tabulations of results in this report.

The least-squares solution for this example does not differ very noticeably from that for Example 1. However, the predicted errors are larger as is evident from a comparison of Tables 3 and 4. The correlation matrix differs in detail from that for Example 1, but it exhibits similar, though somewhat more pronounced, short-range anticorrelation features.

Example 3

The basic parameters defined for Example 1 and the relaxation of all input correlations as for Example 2 are retained for this example. The only exception is that an A_0 consisting of elements which have been altered at random within ±2.8% from the values in Table 1 is assumed. The results of the least-squares analysis for this example appear in Table 5 and Fig. 5. The solution group cross sections are not as close to the actual cross section curve as was the case for Examples 1 and 2. However, except for two groups, the solution is an improvement over the apriori. The calculated uncertainties for the solution are similar to Example 2, and the deviations of the *solution* from the actual group cross sections are within these uncertainties for all groups except the first group where we must allow for the previously-mentioned group approximation errors.

Table 4. Least-Squares Results for Example 2

Group	Apriori σ	Difference	Actual σ	Difference	Solution σ	
1	2 (40%)	+122%	0.9	-22.7%	0.696	(18.6%)
2	3 (33.3%)	+20%	2.5	+5.1%	2.627	(12.3%)
3	5 (30%)	+20.5%	4.15	-2%	4.047	(16.8%)
4	9 (33.3%)	+41.7%	6.35	-2.4%	6.200	(20.4%)
5	12 (25%)	+34.8%	8.9	+4.2%	9.273	(19.5%)
6	14 (28.5%)	+20.7%	11.6	+1.8%	11.813	(21.7%)
7	14 (28.5%)	-2.8%	14.4	-2.6%	14.031	(22.0%)
8	16 (31.3%)	-7.2%	17.25	+3.6%	17.873	(21.8%)
9	17 (29.4%)	-14.4%	19.85	-0.8%	19.687	(21.3%)
10	19 (28.9%)	-14.0%	22.1	+2.1%	22.557	(20.6%)
11	20 (25%)	-16.8%	24.05	-5.3%	22.768	(19.9%)
12	21 (28.6%)	-17.5%	25.45	-5.3%	24.104	(22.7%)
13	20 (30%)	-24.7%	26.55	-17.2%	21.972	(26.1%)
14	22 (31.8%)	-20.1%	27.525	-15.5%	23.261	(29.5%)
15	23 (30.4%)	-18.9%	28.375	-17.6%	23.367	(29.9%)

$(\chi_m^2/m) = 0.50$

Table 5. Least-Squares Results for Example 3

Group	Apriori σ	Difference	Actual σ	Difference	Solution σ	
1	2 (40%)	+122%	0.9	-22.3%	0.699	(18.6%)
2	3 (33.3%)	+20%	2.5	+2.5%	2.563	(12.6%)
3	5 (30%)	+20.5%	4.15	-1.7%	4.079	(16.7%)
4	9 (33.3%)	+41.7%	6.35	+0.5%	6.380	(19.8%)
5	12 (25%)	+34.8%	8.9	+9%	9.701	(18.6%)
6	14 (28.5%)	+20.7%	11.6	-11.4%	10.274	(25%)
7	14 (28.5%)	-2.8%	14.4	-3.7%	13.869	(22.2%)
8	16 (31.3%)	-7.2%	17.25	+17.5%	20.267	(19.2%)
9	17 (29.4%)	-14.4%	19.85	+7.4%	21.310	(19.7%)
10	19 (28.9%)	-14.0%	22.1	+4.2%	23.032	(20.2%)
11	20 (25%)	-16.8%	24.05	-6.6%	22.474	(20.2%)
12	21 (28.6%)	-17.5%	25.45	-5.7%	23.995	(22.8%)
13	20 (30%)	-24.7%	26.55	-16.7%	22.107	(25.9%)
14	22 (31.8%)	-20.1%	27.525	-15.8%	23.169	(29.6%)
15	23 (30.4%)	-18.9%	28.375	-17.8%	23.311	(29.9%)

$(\chi_m^2/m) = 0.65$

Example 4

Most of the parameters from Example 1 and the no-correlation assumption
of Example 2 are used in this example. However, the input utilizes a set of
group fluxes Φ generated by altering individual elements at random within the
established limits of uncertainty. The results from a least-squares analysis
of this problem appear in Table 6 and Fig. 6. The solution is closer to the
actual cross section curve than the apriori for all fifteen groups. Therefore,
the solution is somewhat better than the one obtained in Example 3. This
indicates that the unfolding process is not as sensitive to uncertainties in Φ
as it is to uncertainties in A_0, at least for the physical situation simulated
here. However, it would be imprudent to reach a general conclusion from this
single result. The calculated uncertainties for the solution are similar in
magnitude to those derived for Examples 2 and 3. Except for the lowest group,
the differences between the solution group cross sections and the actual group
cross sections are well within the calculated uncertainties.

Example 5

Once again the assumptions of Example 1 and 2 apply except we now allow
both A_0 and Φ to deviate at random, within the defined uncertainties of this
simulated problem. Other than the fact that input data correlations are
overlooked, this example is the closest to reality of those considered so far
in that it allows for uncertainty of all the parameters which would be experi-
mental quantities in a real situation. The least-squares results which appear
in Table 7 and Fig. 7 offer no surprises. The solution is closer to the
actual cross section curve than is the apriori for all but two groups. Except
for the lowest group, all differences between the solution values and the
actual group cross sections are smaller than the calculated uncertainties.
The calculated uncertainties are everywhere smaller than the apriori uncertain-
ties. This must be so since a basic premise of the method is that the addition
of any new information should to some extent improve our knowledge of the cross
section. The reduction in cross section uncertainty is significant below ~15
MeV, indicating that the contribution made by introducing the new information
is especially valuable at lower energies. Thus we see from a quite-realistic
simulation how a set of new integral results (obtained from measurements
involving generally broad responses) has improved our knowledge of the differ-
ential cross section.

Example 6

Next, we investigate the sensitivity of the solution to the apriori cross
section. The quantities A_0 and Φ are fixed at the same values used in
Example 1, and it is assumed that no correlations exist between the uncertain-
ties for any of the input parameters, as was the case for Example 2. Now,
however, we modify the apriori by selecting a new set of group cross sections
σ which deviate at random from previous values (see Tables 3-7) within the
established uncertainties. This new apriori appears in Table 8 and Fig. 8.
The same percentage uncertainties are assumed for this new apriori as for the

Table 6. Least-Squares Results for Example 4

Group	Apriori σ	Difference	Actual σ	Difference	Solution σ	
1	2 (40%)	+122%	0.9	−23.1%	0.692	(18.4%)
2	3 (33.3%)	+20%	2.5	+10.4%	2.761	(12.5%)
3	5 (30%)	+20.5%	4.15	−6%	3.900	(17.6%)
4	9 (33.3%)	+41.7%	6.35	−6%	5.971	(21.3%)
5	12 (25%)	+34.8%	8.9	+5.9%	9.427	(18.5%)
6	14 (28.5%)	+20.7%	11.6	+3.3%	11.981	(21.2%)
7	14 (28.5%)	−2.8%	14.4	+2.5%	14.753	(−0.7%)
8	16 (31.3%)	−7.2%	17.25	−1.8%	16.943	(22.9%)
9	17 (29.4%)	−14.4%	19.85	−2.3%	19.400	(21.6%)
10	19 (28.9%)	−14.0%	22.1	+2.2%	22.588	(20.7%)
11	20 (25%)	−16.8%	24.05	−4.6%	22.953	(19.6%)
12	21 (28.6%)	−17.5%	25.45	−5.2%	24.121	(22.7%)
13	20 (30%)	−24.7%	26.55	−17%	22.040	(26.%)
14	22 (31.8%)	−20.1%	27.525	−14.1%	23.634	(29%)
15	23 (30.4%)	−18.9%	28.375	−17.6%	23.393	(29.8%)

$(\chi_m^2/m) = 0.56$

Table 7. Least-Squares Results for Example 5

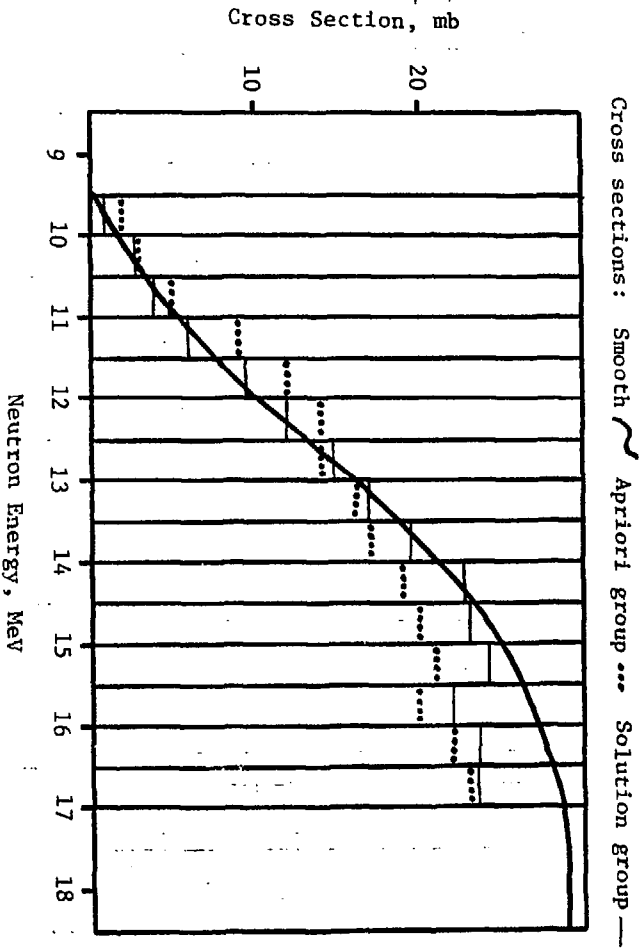| Group	Apriori σ	Difference	Actual σ	Difference	Solution σ	
1	2 (40%)	+122%	0.9	−24.1%	0.683	(18.7%)
2	3 (33.3%)	+20%	2.5	+7.4%	2.684	(12.9%)
3	5 (30%)	+20.5%	4.15	−2.7%	4.038	(17%)
4	9 (33.3%)	+41.7%	6.35	+11.5%	5.620	(22.6%)
5	12 (25%)	+34.8%	8.9	+9.3%	9.730	(17.9%)
6	14 (28.5%)	+20.7%	11.6	+12.5%	13.047	(19.5%)
7	14 (28.5%)	−2.8%	14.4	−5.1%	13.669	(22.3%)
8	16 (31.3%)	−7.2%	17.25	−10.7%	15.409	(25.2%)
9	17 (29.4%)	−14.4%	19.85	−2.2%	19.409	(21.6%)
10	19 (28.9%)	−14.0%	22.1	+1.6%	22.446	(20.8%)
11	20 (25%)	−16.8%	24.05	−7.4%	22.276	(20.2%)
12	21 (28.6%)	−17.5%	25.45	−8.8%	23.219	(23.6%)
13	20 (30%)	−24.7%	26.55	−20%	21.252	(27%)
14	22 (31.8%)	−20.1%	27.525	−16.2%	23.066	(29.7%)
15	23 (30.4%)	−18.9%	28.375	−18.3%	23.180	(30.1%)

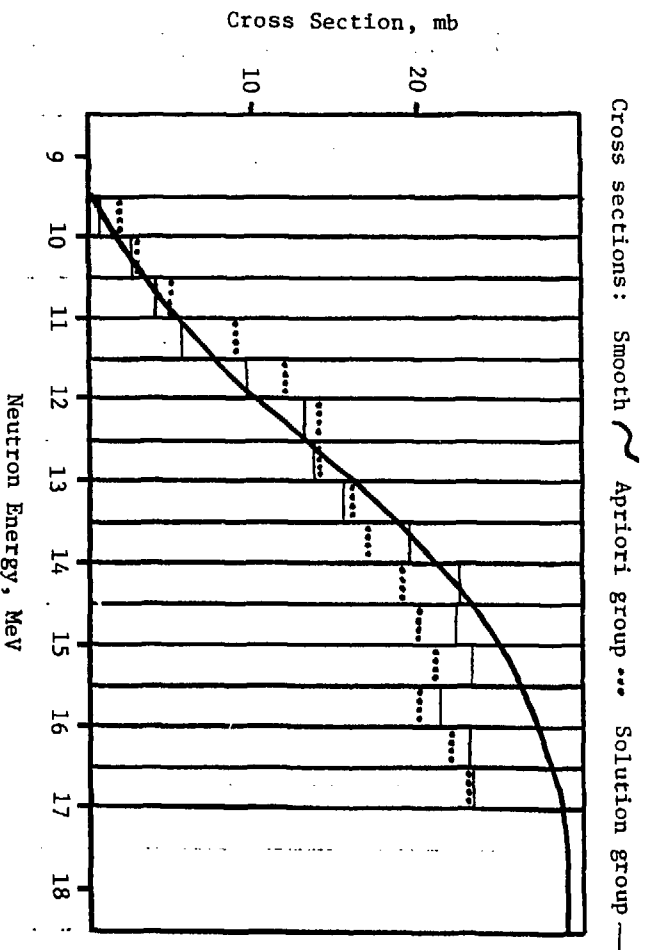$(\chi_m^2/m) = 0.57$

Figure 6: Cross sections for Example 4.

Cross sections: Smooth ⌒ Apriori group ••• Solution group —

Figure 7: Cross sections for Example 5.

Cross sections: Smooth ⌒ Apriori group ••• Solution group —

Table 8. Least-Squares Results for Example 6

Group	Apriori σ	Difference	Actual σ	Difference	Solution σ
1	2.200 (40%)	+144%	0.9	−19.8%	0.722 (19.6%)
2	2.439 (33.3%)	−2.4%	2.5	+2.6%	2.566 (12.4%)
3	4.516 (30%)	+8.8%	4.15	−0.3%	4.139 (15.9%)
4	8.322 (33.3%)	+31.1%	6.35	−9%	5.777 (21.4%)
5	14.630 (25%)	+64.4%	8.9	+16.4%	10.357 (17.5%)
6	13.958 (28.5%)	+20.3%	11.6	+5.2%	12.200 (21.2%)
7	10.266 (28.5%)	−28.7%	14.4	−17.3%	11.906 (25.9%)
8	14.320 (31.3%)	−17%	17.25	−3.2%	16.696 (23.3%)
9	18.539 (29.4%)	−6.6%	19.85	+1.3%	20.106 (20.9%)
10	23.569 (28.9%)	+6.6%	22.1	+11.3%	24.602 (18.9%)
11	24.165 (25%)	+0.5%	24.05	+3.2%	24.812 (18.3%)
12	21.893 (28.6%)	−14%	25.45	−10.8%	22.697 (24.1%)
13	25.089 (30%)	−5.5%	26.55	−3.4%	25.637 (22.4%)
14	26.634 (31.8%)	−3.2%	27.525	−1.9%	26.984 (25.5%)
15	26.496 (30.4%)	−6.6%	28.375	−6.3%	26.599 (26.2%)

$(\chi_m^2/m) = 0.54$

Table 9. Least-Squares Results for Example 7

Group	Apriori σ	Difference	Actual σ	Difference	Solution σ
1	0.7 (10%)	−22.2%	0.9	−25.8%	0.668 (5.9%)
2	2.6 (10%)	+4%	2.5	+8.1%	2.702 (6.1%)
3	3.7 (10%)	−10.8%	4.15	−8.8%	3.784 (7.6%)
4	6.3 (10%)	−0.8%	6.35	−0.5%	6.318 (7.9%)
5	8.9 (10%)	0	8.9	+3.1%	9.172 (7.9%)
6	11.2 (10%)	−3.4%	11.6	−0.3%	11.571 (8.3%)
7	13.7 (10%)	−4.9%	14.4	−5.1%	13.666 (8.9%)
8	16.7 (10%)	−3.2%	17.25	−7.3%	15.996 (9.4%)
9	21.8 (8%)	+9.8%	19.85	+6.8%	21.201 (7.6%)
10	22 (8%)	−0.5%	22.1	−2.7%	21.496 (7.8%)
11	25 (8%)	+4%	24.05	+1.6%	24.426 (7.9%)
12	26 (8%)	+2.2%	25.45	+0.5%	25.569 (8%)
13	27 (8%)	+1.7%	26.55	+0.6%	26.718 (8%)
14	28 (8%)	+1.7%	27.525	+1.3%	27.886 (8%)
15	30 (8%)	+5.7%	28.375	+5.6%	29.956 (8%)

$(\chi_m^2/m) = 0.33$

-31-

Cross sections: Smooth $\sim$ Apriori group ••• Solution group —
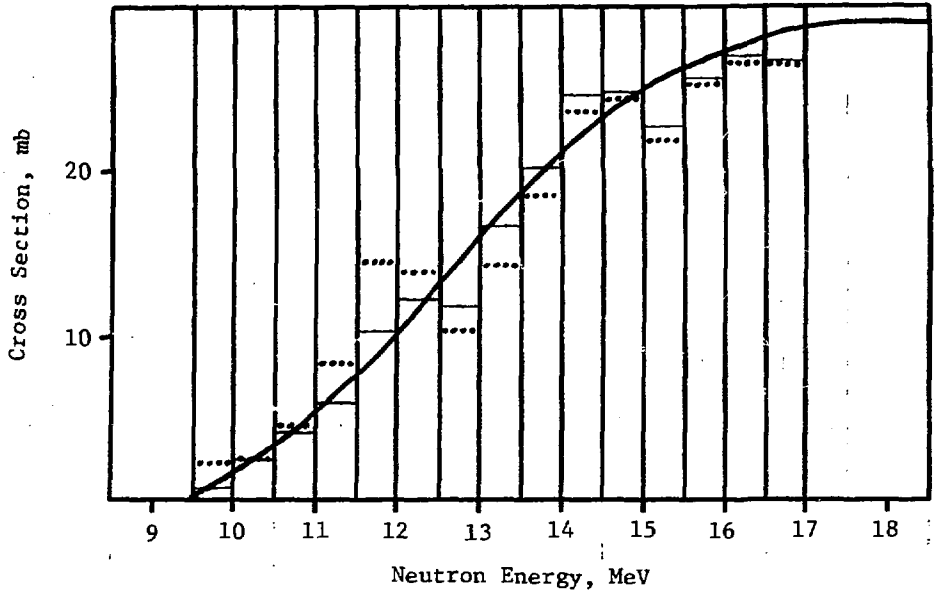

Figure 8: Cross sections for Example 6.

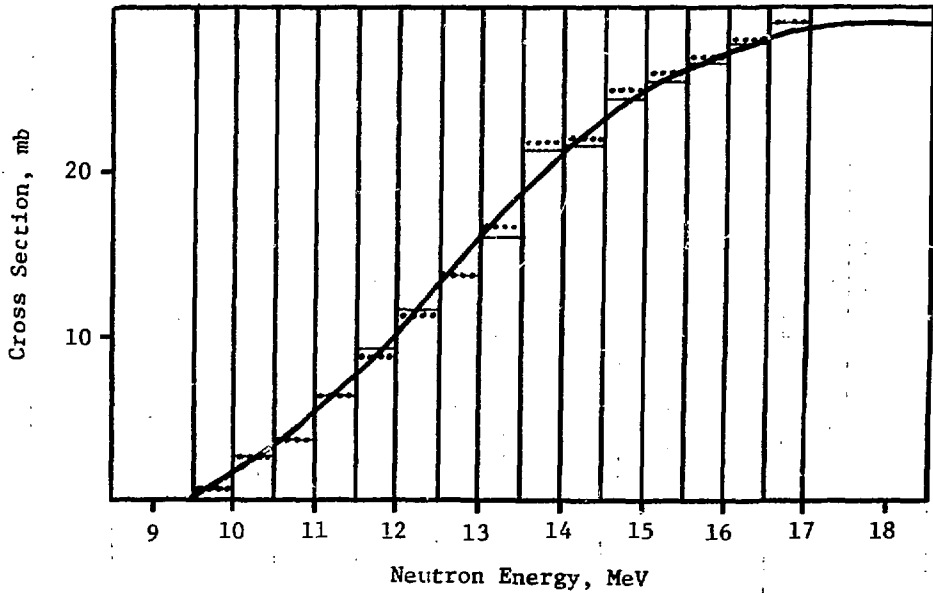Cross sections: Smooth $\sim$ Apriori group ••• Solution group —

Figure 9: Cross sections for Example 7.

previous one. We see from Fig. 8 that the apriori generated by this method is not very physically realistic. The results of this analysis should be compared with Example 2 because the only difference in these two problems is the choice of the apriori cross section. The results of the least-squares analysis appear in Table 8 and Fig. 8. There are indeed some differences between the present results and Example 2. This has to be the case since the least-squares algorithm generates what amounts to a complicated weighted average of the new and apriori information. Nevertheless, the solution here is still clearly superior to the apriori, offering a smaller deviation from the actual cross section curve for all but two groups. Again, the differences are smaller than the derived uncertainties for all but the lowest group. It is evident that the solution tends to follow the apriori for the upper energy groups, and by chance the apriori is closer to the actual cross section curve in this region than was the apriori used in Examples 1 to 5. The magnitudes of the computed uncertainties are consistent with the preceding Examples 2 through 5.

The present example is somewhat artificial since the choice of an apriori should <u>not</u> be an arbitrary matter. the apriori should – in fact <u>must</u> – represent the best available prior knowledge of the cross section. Otherwise the algorithm is improperly applied. Even if <u>no</u> prior experimental data are available for a particular reaction, the investigator must introduce a rational apriori which represents an estimate based on systematic considerations or on a model calculation.

Example 7

The assumed uncertainties for the apriori cross sections in each of the preceeding six examples were all rather large, so the new simulated experimental information was able to contribute significantly toward improving our knowledge of the cross section. Now we will consider an example in which the apriori does not differ very much from the actual group cross section set and the assumed apriori uncertainties are considerably smaller than before. Otherwise, the conditions are identical to Example 5, with A_0 and Φ varied at random from the normal values defined in Example 1. The results of this analysis appear in Table 9 and Fig. 9. For nine out of fifteen of the groups, the solution represents an improvement over the apriori. Also, the calculated uncertainties are somewhat smaller than the apriori uncertainties. The differences between the solution and the actual group cross section values are smaller than the calculated uncertainties for all groups except the lowest three where the error resulting from the group approximation is quite evident. However, the contribution of the new data is really not too significant in this hypothetical example. This example thus illustrates the situation where performance of a new measurement is of dubious merit. One attractive feature of the least-squares algorithm is that it provides an unbiased assessment of the value of any new measurement from the point of view of improving knowledge of a specific cross section set.

Example 8

For all of the preceding examples we introduced apriori cross sections for which it was assumed that no correlations existed for the apriori cross-section

uncertainties. In the present example we consider an opposite extreme, namely the situation where it is assumed that we know the shape of the cross section very well but are uncertain about the normalization. For this simulation we again select conditions as specified in Example 5, except that we introduce an apriori which indicates the same general shape as the actual cross section curve, except for the lowest three groups where approximation errors are involved. Here, the introduced apriori cross sections are generally ~25% too large and uncertainties of 25% are assumed for each element of the apriori, with a correlation condition of 100%. The results of the analysis appear in Table 10 and Fig. 10. If we neglect the three lowest groups, it is seen that the solution cross sections are very close to the actual group cross sections, and the calculated uncertainties are very small. Imposition of the 100%-correlation assumption prevents the algorithm from adjusting the shape. Therefore, all of the integral measurements contribute redundantly toward securing the proper normalization. The solution correlation matrix also indicates 100% correlation, as indeed it must. It is reassuring that the algorithm performs properly for this physically-transparent situation.

Example 9

In this example we investigate a pathological situation in order to see whether the algorithm provides a suitable warning. Consider the physical problem as stated in Example 5. However, now we introduce an apriori with 30% uncertainties for all groups, with 100% correlations assumed. Effectively we are stating, as in Example 8, that we know the shape but are uncertain about the normalization. The difference here is that we introduce an apriori with a very wrong shape. One should be skeptical of an apriori having these properties for several reasons. First, if the apriori is based upon a single comprehensive measurement, one is not protected against the possibility that a systematic blunder produced a shape error. The reliability of an evaluation based upon a single experiment is always subject to question. While the 30% uncertainty may reasonably reflect the normalization inadequacy, the assumption of 100% correlation is unrealistic in that it implicitly overstates the certainty to which the cross section shape is known. This situation poses a dilemma which is all too familiar to evaluators. Of course, it could be that the nature of this single experiment strongly implies that the error should be predominently in the normalization rather than in the shape. On the other hand, suppose the evaluation used as the apriori is based on several data sets. Then, it is very unlikely that the evaluation would assume the form described above. The only plausible scenario which would lead all the experiments to generate results with the same wrong shape would be one in which all the experiments used a common erroneous standard. A competent evaluator would recognize this and have a close look at the suspicious standard. It is important for evaluators to have a close look at the details of all the experiments which produce the data they are to evaluate.

While dwelling on the subject of wrong shapes and strong uncertainty correlations, it is worthwhile to comment on what appears to this author to be a severe potential problem associated with the use of model calculations to provide apriori cross section sets. An inadequate or improperly-parameterized model can certainly lead to prediction of a wrong shape for a cross section.

Table 10. Least-Squares Results for Example 8

Group	Apriori σ		Difference	Actual σ	Difference	Solution σ	
1	0.82	(25%)	−8.9%	0.9	−27.9%	0.649	(1.5%)
2	3.36	(25%)	+34.4%	2.5	+6.4%	2.660	(1.5%)
3	4.92	(25%)	+18.6%	4.15	−6.1%	3.895	(1.5%)
4	8.07	(25%)	+27.1%	6.35	+0.6%	6.389	(1.5%)
5	11.1	(25%)	+24.7%	8.9	−1.3%	8.787	(1.5%)
6	14.5	(25%)	+25%	11.6	−1%	11.479	(1.5%)
7	18.1	(25%)	+25.7%	14.4	−0.5%	14.329	(1.5%)
8	21.3	(25%)	+23.5%	17.25	−2.2%	16.862	(1.5%)
9	25	(25%)	+25.9%	19.85	−0.3%	19.791	(1.5%)
10	27.3	(25%)	+23.5%	22.10	−2.2%	21.612	(1.5%)
11	30.3	(25%)	+26%	24.05	−0.3%	23.987	(1.5%)
12	31.9	(25%)	+25.3%	25.45	−0.8%	25.253	(1.5%)
13	33.1	(25%)	+24.7%	26.55	−1.3%	26.203	(1.5%)
14	34.3	(25%)	+24.6%	27.525	−1.3%	27.153	(1.5%)
15	35.6	(25%)	+25.5%	28.375	−0.7%	28.182	(1.5%)

$(\chi_m^2/m) = 0.29$

Table 11. Least-Squares Results for Example 9

Group	Apriori σ		Difference	Actual σ	Difference	Solution σ	
1	1	(30%)	+11.1%	0.9	+5.9%	0.953	(1.4%)
2	4	(30%)	+60%	2.5	+52.5%	3.812	(1.4%)
3	6	(30%)	+44.6%	4.15	+37.8%	5.717	(1.4%)
4	7	(30%)	+10.2%	6.35	+5%	6.670	(1.4%)
5	8.5	(30%)	−4.5%	8.9	−9%	8.100	(1.4%)
6	10	(30%)	−13.8%	11.6	−17.9%	9.529	(1.4%)
7	12	(30%)	+16.7%	14.4	−20.6%	11.435	(1.4%)
8	14	(30%)	−18.8%	17.25	−22.7%	13.341	(1.4%)
9	16	(30%)	−19.4%	19.85	−23.2%	15.247	(1.4%)
10	17	(30%)	−23.1%	22.1	−26.7%	16.199	(1.4%)
11	19	(30%)	−21%	24.05	−24.7%	18.105	(1.4%)
12	20	(30%)	−21.4%	25.45	−25.1%	19.058	(1.4%)
13	20	(30%)	−24.7%	26.55	−28.2%	19.058	(1.4%)
14	21	(30%)	−23.7%	27.525	−27.3%	20.011	(1.4%)
15	21	(30%)	−26%	28.375	−29.5%	20.011	(1.4%)

$(\chi_m^2/m) = 13.63$

Cross sections: Smooth ⌢ Apriori group ••• Solution group ——

Apriori values for
Groups 12-15 are
off scale and thus
not shown. See Table
10.

Neutron Energy, MeV
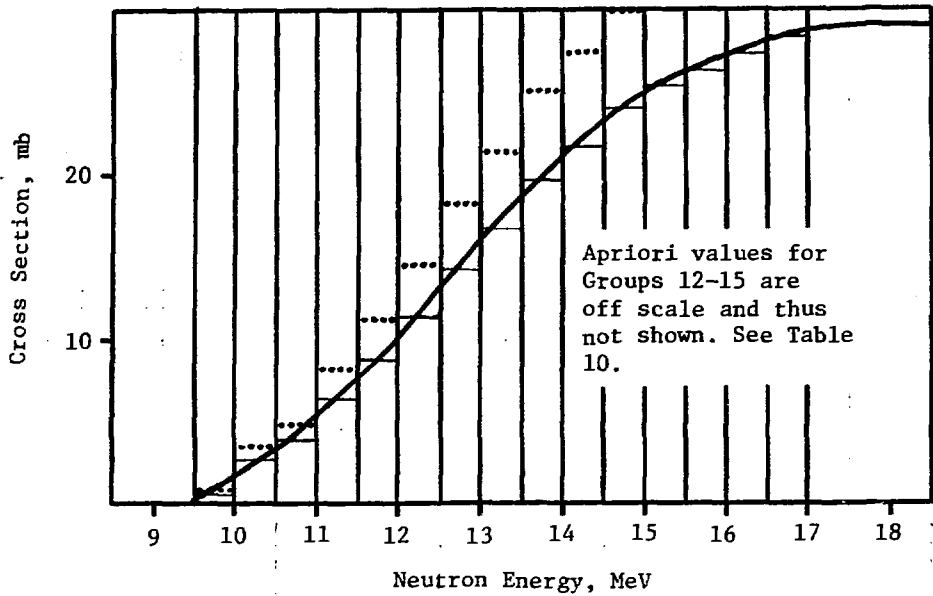
Figure 10: Cross sections for Example 8.

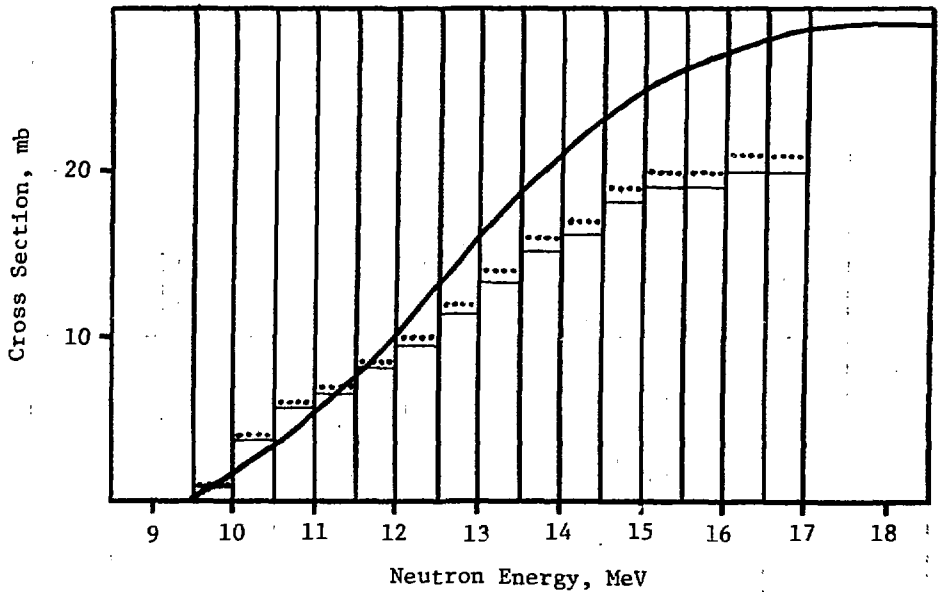Cross sections: Smooth ⌢ Apriori group ••• Solution group ——

Neutron Energy, MeV

Figure 11: Cross sections for Example 9.

At the same time, it is a feature of models that one tends to calculate a large number of cross section from far fewer parameters, with the result that the predicted cross section uncertainties may well be very strongly correlated [11,13]. Once strong correlations become imbedded into the problem via the apriori, it is apparent that it is difficult to remove them by the addition of new experimental information. This important point can be emphasized by a metaphor: "once the salt is in the soup, it cannot be removed."

We assume that our hypothetical experimenter is not aware of such hidden problems when he obtains the present apriori from an evaluated data file. He proceeds to analyze the new integral data set in consort with this apriori. The results of the analysis appear in Table 11 and Fig. 11. Since we know the true cross section, we see immediately what has happened from Fig. 11: The apriori has the wrong shape and the least-squares algorithm is not permitted to adjust the shape because of the severe constraint imposed by the assumption of 100% correlation for the apriori uncertainties. Therefore, the algorithm finds a local minimum which is not near the actual cross section. The results in Table 11 are more revealing to our blind experimenter who is not privileged to know the actual cross section. The calculated minimum chi-square per degree of freedom is 13.63. The experimenter immediately sees that the input information for the least-squares problem is highly improbable and knows he must proceed to investigate the discrepancy. As discussed by Perey, more detailed investigation of specific terms from Eq. (45), which is utilized to calculate χ^2_m, can also often be revealing [4]. In addition to carefully reviewing his own experiment, the researcher should not neglect to trace the origin of the apriori, which we happen to know is the true offender in this example. The solution indicated in Table 11 and Fig. 11 is mathematically correct for the problem as posed, but in this example we have been misled by erroneous input information and thus must reject the solution.

Example 10

The hypothetical neutron spectra from Fig. 2, which are involved in all the preceeding examples, are seen to be of limited usefulness in providing information about the cross section above 14-15 MeV, except for the special case where we have a good prior knowledge of the shape. Our hypothetical experimenter may consider that the cross section $\sigma(E)$ is large enough in this energy range so that measurements with less-intense nearly-monoenergetic neutron sources are feasible. Therefore, he decides to enlarge the scope of his experiment by performing three monoenergetic measurements at 14.75, 15.75 and 16.75 MeV, respectively. Assume that all the information stated in Example 1 is used here, and that m is increased from 15 to 18 to account for the additional measurements in spectra $\phi_{16}(E)$, $\phi_{17}(E)$ and $\phi_{18}(E)$. For simplicity, we assume these to be Gaussians represented by

$$\phi_i(E) = \psi_i \exp\left[-\beta_i^2 (E - E_i)^2\right], \tag{58}$$

$$\beta_i = 2 (\ln 2)^{1/2}/\Delta E_i, \tag{59}$$

for i = 16, 17 and 18. The E_i are the above-mentioned energies. The ΔE_i (full-width at half maximum of the Gaussian) are all assumed to be 0.2 MeV. The assumed values ψ_i are: $\psi_{16} = 5000.0$, $\psi_{17} = 10000.0$ and $\psi_{18} = 15000.0$. Equations (58) and (59) are used to calculate the needed extra elements of Φ which is now expanded from a 15x15 matrix to an 18x15 matrix (270 elements). The uncertainties for these additional group fluxes are calculated as discussed in Example 1. The three additional reaction yields to be added to A_0 are calculated by numerical integration of Eq. (30) and the following values (with assumed 2.8% uncertainties which are 50% correlated to all other a_{oi} uncertainties) are obtained: $a_{o,16} = 25600.0$ $a_{o,17} = 56523.0$ and $a_{o,18} = 90463.0$. The least-squares solution for this example appears in Table 12 and Fig. 12.

The solution group cross sections and calculated uncertainties are not very different from Example 1 except for Groups 11, 13 and 15. Essentially all of the response to the monoenergetic measurements appears in these groups. The result is that there the corresponding solution values approach the actual cross section curve quite closely and the calculated uncertainties are small. The monoenergetic results tend to override the influence of the apriori, but the effect is localized to the specific groups addressed by the monoenergetic data. The influence of the monoenergetic results does not spread to neighboring groups because the uncertainties for the apriori in this example are assumed to be uncorrelated. In other words, no preconceived notion of the shape is introduced and the monoenergetic data only influence the cross section over narrow energy ranges which do not extend beyond their corresponding groups. Clearly, the monoenergetic data enhance our knowledge of the cross section relative to the outcome of Example 1. Our experimenter should have made even more measurements of this nature so that response coverage would have been provided for each of the groups above ~14 MeV in order to compensate for the inadequacy of the broad-spectrum experiment relative to the high-energy region.

Example 11

Next consider an example which is identical to Example 10 in all respects except for the assumed correlations of the apriori cross section uncertainties. This time we introduce an assumption of short-range correlations of moderate strength by means of the formula

$$(C_\sigma)_{ij} = \begin{cases} 1 - \dfrac{|i-j|}{2} & \text{for } |i-j| < 2, \\ \\ 0 & \text{otherwise,} \end{cases} \qquad (i, j = 1,15). \qquad (60)$$

Thus, for this apriori all group cross section uncertainties are uncorrelated to other members of the set, except for adjacent groups where the correlation is 50%. The results appear in Table 13 and Fig. 13, and they are quite remarkable. Compared to the solution from Example 10, the solution here is far closer to the actual cross section and the calculated errors are noticeably smaller. Except for the lowest-energy group, the solution group cross sections differ from the actual group cross sections by considerably less than

Table 12. Least-Squares Results for Example 10

Group	Apriori σ		Difference	Actual σ	Difference	Solution σ	
1	2	(40%)	+122%	0.9	-21.8%	0.704	(18.6%)
2	3	(33.3%)	+20%	2.5	+6.3%	2.658	(8.2%)
3	5	(30%)	+20.5%	4.15	-2.8%	4.034	(12.9%)
4	9	(33.3%)	+41.7%	6.35	-0.3%	6.332	(15.7%)
5	12	(25%)	+34.8%	8.9	+1.9%	9.069	(16.3%)
6	14	(28.5%)	+20.7%	11.6	+0.9%	11.706	(19.3%)
7	14	(28.5%)	-2.8%	14.4	-2.4%	14.048	(20.2%)
8	16	(31.3%)	-7.2%	17.25	+2.8%	17.725	(20.6%)
9	17	(29.4%)	-14.4%	19.85	-1.7%	19.508	(20.7%)
10	19	(28.9%)	-14.0%	22.1	+0.6%	22.243	(19.2%)
11	20	(25%)	-16.8%	24.05	-0.6%	23.899	(4.4%)
12	21	(28.6%)	-17.5%	25.45	-6.7%	23.749	(21%)
13	20	(30%)	-24.7%	26.55	-0.7%	26.366	(3.9%)
14	22	(31.8%)	-20.1%	27.525	-16%	23.126	(29.2%)
15	23	(30.4%)	-18.9%	28.375	-0.6%	28.200	(3.9%)

$(\chi_m^2/m) = 0.50$

Table 13. Least-Squares Results for Example 11

Group	Apriori σ		Difference	Actual σ	Difference	Solution σ	
1	2	(40%)	+122%	0.9	-19.2%	0.727	(17.6%)
2	3	(33.3%)	+20%	2.5	+2.4%	2.560	(7.6%)
3	5	(30%)	+20.5%	4.15	+3.1%	4.277	(9.3%)
4	9	(33.3%)	+41.7%	6.35	-5.4%	6.007	(12.4%)
5	12	(25%)	+34.8%	8.9	+4.6%	9.305	(10.9%)
6	14	(28.5%)	+20.7%	11.6	+0.1%	11.608	(13.4%)
7	14	(28.5%)	-2.8%	14.4	-2.7%	14.011	(14%)
8	16	(31.3%)	-7.2%	17.25	+2.5%	17.675	(15.4%)
9	17	(29.4%)	-14.4%	19.85	-4.6%	18.941	(12.4%)
10	19	(28.9%)	-14.0%	22.1	+1.1%	22.340	(15.6%)
11	20	(25%)	-16.8%	24.05	-0.8%	23.846	(4.4%)
12	21	(28.6%)	-17.5%	25.45	+3.1%	26.248	(15.6%)
13	20	(30%)	-24.7%	26.55	-0.9%	26.324	(3.9%)
14	22	(31.8%)	-20.1%	27.525	+2.6%	28.248	(17.6%)
15	23	(30.4%)	-18.9%	28.375	-0.7%	28.180	(3.9%)

$(\chi_m^2/m) = 0.42$

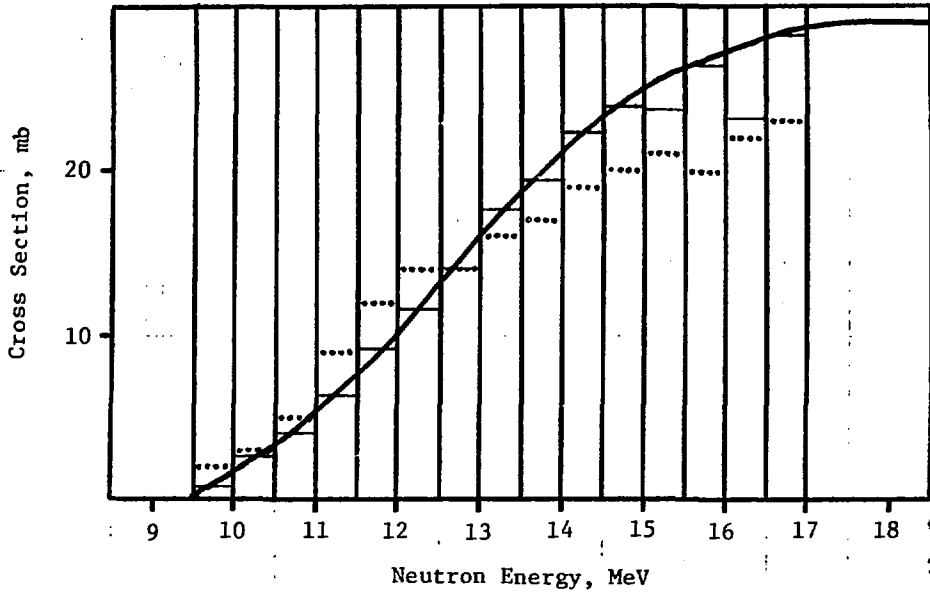Cross sections: Smooth $\curvearrowright$ Apriori group ••• Solution group ——

Figure 12: Cross sections for Example 10.

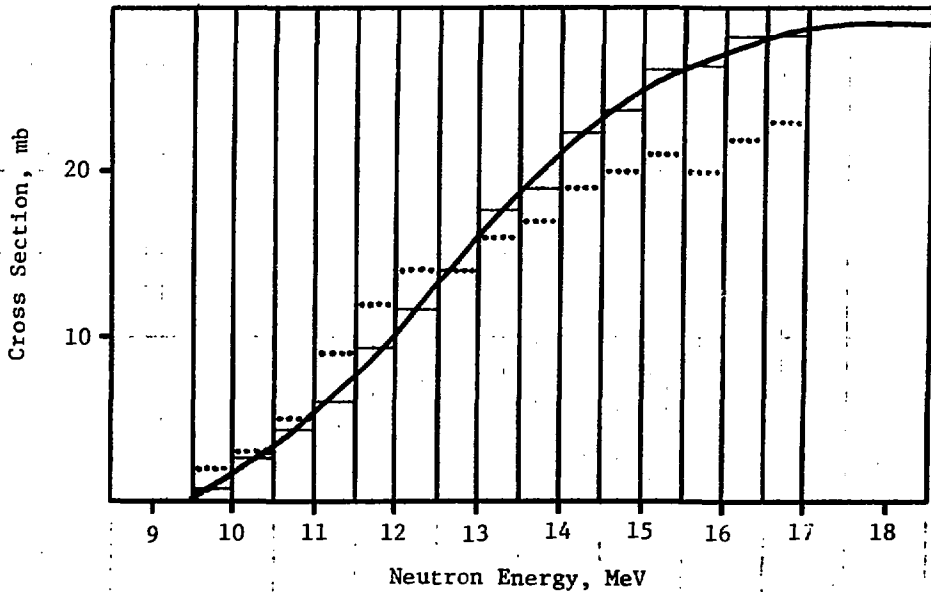Cross sections: Smooth $\curvearrowright$ Apriori group ••• Solution group ——

Figure 13: Cross sections for Example 11.

the derived uncertainties. Apparently the combined broad-group and monoenergetic measurements led to a significantly improved understanding of the cross section. Actually the simulated experiment here is identical to that for Example 10 so the measurer cannot take credit for the apparently greater impact of his data in this example than in the previous one. The difference is obviously traceable to the apriori. By including a correlation condition such as the one defined by Eq. (60), it is indicated that our prior knowledge of the cross section is far more definitive in this example than it was for Example 10. Furthermore, the correlation condition here does not introduce any constraints which turn out to be at odds with the physical realities of the problem, as was the case for Example 9. Equation (60) states that when we adjust the cross section we are required to move adjacent groups together to some extent (50% correlation). Since the apriori as given implies a generally monotonically increasing cross section with energy, consistent with the actual cross section shape, the adjustment process can actually use the correlation constraint to advantage in minimizing χ^2. Said another way, this particular constraint effectively reduces the problem's degrees of freedom without blocking any paths in parameter space which lead toward a mathematical minimum of χ^2 near the actual cross section.

We are investigating simulated problems in this report and thus are at liberty to make various assumptions about the apriori for educational purposes. The reader must by now be fully aware of the fact that apriori cross sections cannot be arbitrarily selected when applying the least-squares algorithm. In fact, the apriori is dictated by the research history associated with the physical cross section in question, for all practical purposes.

Example 12

For our last example we consider an experiment involving the set of fifteen multiple-group spectra shown in Fig. 14. For mathematical convenience the various discrete groups have been represented by Gaussians according to Eqs. (58) and (59). Most of the peak centroids E_i correspond to group midpoint energies. The peak widths ΔE_i are in the range 0.2 to 1.7 MeV and the peak amplitudes ψ_i are in the range 1000.0 to 10000.0. These spectra are characteristic of what might be obtained using a typical neutron-producing reaction and thin targets. The narrow discrete groups correspond to individual resolved levels in the product nucleus while the broad groups simulate what might result from the excitation of several unresolved levels. The situation here is like that discussed in the portion of Section II between Eqs. (11) and (21), except it is apparent that there is no single dominant group for spectra $\phi_4(E)$ through $\phi_{15}(E)$. A set of group fluxes Φ is calculated from these spectra and a covariance matrix is generated in the manner described in Section II and in Example 1. A set of calculated reaction yields A_0 is also generated, using the cross section from Fig. 3.A and the Gaussian parameters corresponding to Fig. 14. These a_{0i} are listed in Table 14. An uncertainty of 2.8% is assumed for these elements of A_0 and the off-diagonal correlations are set at 50%. Finally, the same apriori cross section as was used in Example 1 is introduced. The results of the analysis appear in Table 15 and Fig. 15. The solution cross sections are quite close to the actual group cross sections for all but the two highest-energy groups. Clearly, the new
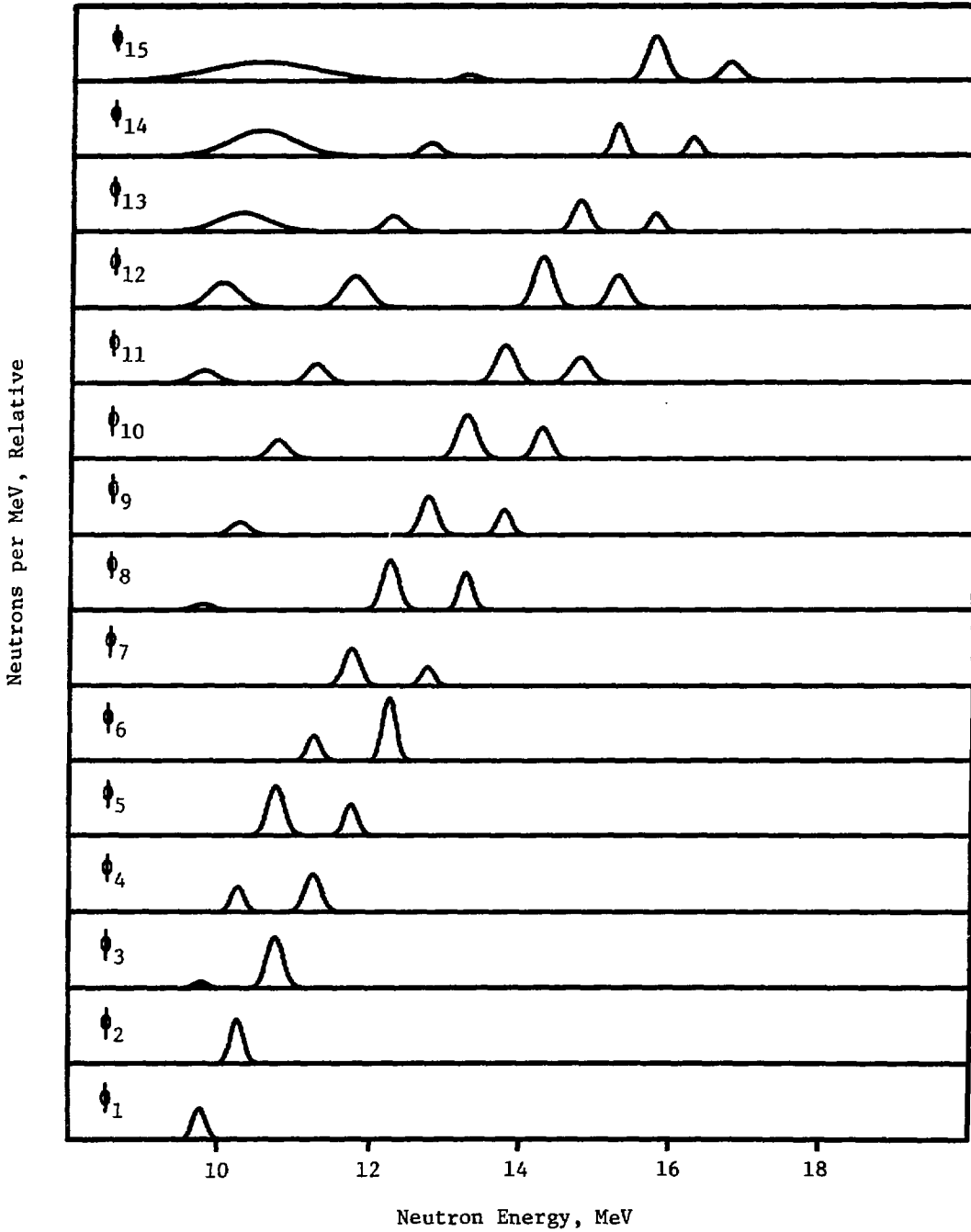
Figure 14: Plots of multiple-group spectra $\phi_i(E)$ used in Example 12.

Table 14. Simulated Reaction Yields for Example 12

Spectrum[a] Index	a_{oi}[b]	Spectrum[a] Index	a_{oi}[b]
1	958.14	9	41493.0
2	3725.6	10	71941.0
3	9028.3	11	75611.0
4	12269.0	12	119740.0
5	18310.0	13	64648.0
6	30103.0	14	68258.0
7	23408.0	15	111090.0
8	47019.0		

[a]Identifies specific ϕ_i from Fig. 14.

[b]Derived from spectrum ϕ_i and σ given in Fig. 3.A, using Eq. (30).

Table 15. Least-Squares Results for Example 12

Group	Apriori σ		Difference	Actual σ	Difference	Solution σ	
1	2	(40%)	+122%	0.9	+0.4%	0.904	(9.7%)
2	3	(33.3%)	+20%	2.5	−0.2%	2.495	(5.4%)
3	5	(30%)	+20.5%	4.15	−0.4%	4.134	(5.1%)
4	9	(33.3%)	+41.7%	6.35	+0.1%	6.358	(6.3%)
5	12	(25%)	+34.8%	8.9	+0.4%	8.936	(6.5%)
6	14	(28.5%)	+20.7%	11.6	−0.4%	11.549	(5.3%)
7	14	(28.5%)	−2.8%	14.4	−1%	14.263	(7.1%)
8	16	(31.3%)	−7.2%	17.25	+0.1%	17.269	(6.5%)
9	17	(29.4%)	−14.4%	19.85	Negligible	19.858	(7.5%)
10	19	(28.9%)	−14.0%	22.1	−2%	21.667	(8.2%)
11	20	(25%)	−16.8%	24.05	−2.1%	23.535	(7.4%)
12	21	(28.6%)	−17.5%	25.45	+1.3%	25.769	(10.8%)
13	20	(30%)	−24.7%	26.55	+1.3%	26.896	(10.3%)
14	22	(31.8%)	−20.1%	27.525	−5.9%	25.884	(18.3%)
15	23	(30.4%)	−18.9%	28.375	−7.2%	26.333	(22.7%)

$(\chi_m^2/m) = 0.57$
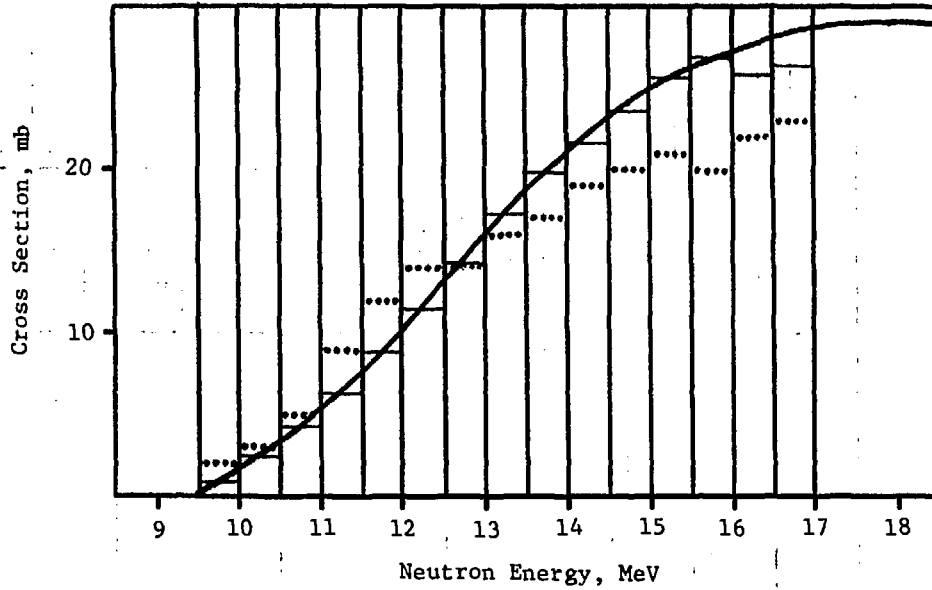
Figure 15: Cross sections for Example 12.

simulated data have more influence over the least-squares process than the apriori for most of the energy range of interest. This is accentuated by a significant reduction in uncertainty for all but the two highest-energy groups. The reason why the new results do not have a greater impact on the highest-energy groups is that for measurements involving spectra $\phi_{14}(E)$ and $\phi_{15}(E)$, most of the strength contributed to $a_{o,14}$ and $a_{o,15}$ comes from lower-energy groups. Therefore these calculated yields are not too sensitive to the higher-energy cross sections. Furthermore, there is no redundancy to add some weight to this energy region. A similar - but even more pronounced - effect is evident for measurements in the spectra from Fig. 2, as discussed in Examples 1 through 9.

IV. CONCLUSION

The examples which appear in Section III demonstrate rather convincingly that the least—squares algorithm is a viable method for deriving differential cross section information from a variety of experimental data. The two advantages which are not generally offered by other methods are:

(i) Experimenters are not restricted to measurements with monoenergetic or nearly—monoenergetic neutron sources. Useful information can also be gained from measurements involving a variety of neutron sources with multiple—group or even continuous—neutron spectra.

(ii) The least—squares method forces one to view nuclear data problems from a much broader perspective. One must examine the prior state of knowledge in addition to performing a specific new experiment. The consistency of the prior and new information is then tested by the algorithm. Finally, one observes from the solution the extent to which the new information added to the overall knowledge of the cross section. If no significant reduction in uncertainties resulted, then the new experiment contributed rather little.

A legitimate argument could be made to the effect that trained evaluators should perform the least—squares analysis described in this paper and not experimenters. This does not in any way alter the mathematical foundation of the method. It simply means that the experimenter would report only the measured information consisting of spectral representations and reaction yield parameters, along with appropriate covariance information. This issue is beyond the scope of this paper.

The importance of the apriori in this process cannot be over emphasized. The most serious risk associated with the approach discussed in this paper is that the impact of a good new experiment may be lost by essentially averaging it with a faulty apriori. Conceivably, the reverse situation could also take place. Namely, a new heavily—weighted erroneous data set could undermine a reasonable understanding of the cross section as embodied in the apriori. This risk has always existed; it is not an intrinsic feature of this method alone. Fortunately, this algorithm yields a chi—square parameter which serves to warn of pathological problems of this nature. There is no doubt that such situations will arise, and they will have to be dealt with on an individual basis.

REFERENCES

1. R. W. Peele, "Requirements on Experiment Reporting to Meet Evaluation Needs," Proceedings of the NEANDC/NEACRP Specialists Meeting on Fast Neutron Fission Cross Sections of U-233, U-235, U-238, and Pu-239," June 28-30, 1976 at Argonne National Laboratory, edited by W. P. Poenitz and A. B. Smith, p. 421, Report Nos. ANL-76-90 or NEANDC (US)-199/L (1976).

2. F. G. Perey, "Least-Squares Dosimetry Unfolding: The Program STAY'SL," ORNL/TM-6062, Oak Ridge National Laboratory, Oak Ridge, TN 37830 (1977).

3. F. Schmittroth, "Generalized Least-Squares for Data Analysis," HEDL-TME 77-51, UC-79d, Hanford Engineering Development Laboratory, Richland, Washington (1978).

4. F. G. Perey, "Contributions to Few-Channel Spectrum Unfolding," Report No. ORNL/TM-6267, Oak Ridge National Laboratory, Oak Ridge, TN 37830 (1978).

5. F. G. Perey, "Covariance Matrices of Experimental Data," Proceedings of an International Conference on Neutron Physics and Nuclear Data for Reactors, Harwell, United Kingdom, p. 104 (September 1978).

6. F. Schmittroth, "A Method for Data Evaluation with Lognormal Distributions," Nucl. Sci. Eng. 72, 19 (1979).

7. S. Tagesen, H. Vonach and B. Strohmaier, "Evaluations of the Cross Sections for the Reactions $^{24}Mg(n,p)^{24}Na$, $^{64}Zn(n,p)^{64}Cu$, $^{63}Cu(n,2n)^{62}Cu$ and $^{90}Zr(n,2n)^{89}Zr$, Physics Data 13-1 (1979).

8. A. Allisy, "Some Statistical Methods Used in Metrology," Proceedings of the International School of Physics "Enrico Fermi," course LXVIII, ed. A. Ferro Milone and P. Giacomo, 12-24 July 1976, North-Holland Publishing Company, Amsterdam (1980).

9. W. Mannhart and F. G. Perey, "Covariance Matrices of Cf-252 Spectrum Averaged Cross Sections," Proc. Third ASTM-EURATOM Symposium on Reactor Dosimetry, Ispra, Italy, Oct. 1-5, 1979, Report EUR-6813, Vol. II, p. 1016 (1980).

10. W. Mannhart, "A Small Guide to Generating Covariances of Experimental Data," PTB-FMRB-84, Physikalisch - Technische Bundesanstalt, Braunschweig, Federal Republic of Germany (1981).

11. Donald L. Smith, "Covariance Matrices and Applications to the Field of Nuclear Data," ANL/NDM-62, Argonne National Laboratory, Argonne, Illinois, 60439, U.S.A. (1981).

12. W. P. Poenitz, "Data Interpretation, Objective Evaluation Procedures and Mathematical Techniques for the Evaluation of Energy-Dependent Ratio, Shape and Cross Section Data," Proceedings of the Conference on Nuclear Data Evaluation Methods and Procedures, September 22-25, 1980 at Brookhaven National Laboratory, edited by B. A. Magurno and S. Pearlstein, Report Nos. BNL-NCS-51363 or NEANDC(US)-209, Vol. I, p. 249 (March 1981).

13. Donald L. Smith, "Non-Evaluation Applications for Covariance Matrices," ANL/NDM-67, Argonne National Laboratory, Argonne, IL 60439, U.S.A. (1982).

14. R. Peele, "Uncertainty in the Nuclear Data used for Reactor Calculations," to be published in <u>Sensitivity and Uncertainty Analysis of Reactor Performance Parameters</u>, ed. C. Weisbin. This monograph will be part of the series entitled "Advances in Nuclear Science and Technology" published by Pergamon Press, Oxford, U.K. The author can be contacted at: Engineering Physics Division, Oak Ridge National Laboratory, P.O. Box X, Oak Ridge, Tennessee 37830, U.S.A.

15. R. W. Peele and and T. W. Burrows, "An Annotated Bibliography Covering Generation and Use of Evaluated Cross Section Uncertainty Files (to be published). A preprint can be obtained by contacting R. W. Peele, Engineering Physics Division, Oak Ridge National Laboratory, P.O. Box X, Oak Ridge, Tennessee 37830.

16. Donald L. Smith, "Remarks Concerning the Accurate Measurement of Differential Cross Sections for Threshold Reactions Used in Fast-Neutron Dosimetry for Fission Reactors," ANL/NDM-23, Argonne National Laboratory, Argonne, Illinois 60439, U.S.A. (1976).

17. "Proceedings of the IAEA Consultant's Meeting on Neutron Source Properties", 17-21 March 1980, Debrecen, Hungary, ed. K. Okamoto, INDC (NDS) - 114/GT, IAEA Nuclear Data Section, International Atomic Energy Agency, Vienna, Austria (1980).

18. Donald L. Smith, "Some Comments on Resolution and the Analysis and Interpretation of Experimental Results from Differential Neutron Measurements," ANL/NDM-49, Argonne National Laboratory, Argonne, Illinois 60439, U.S.A. (1979).

19. D. I. Garber and R. R. Kinsey, "Neutron Cross Sections, Vol. II, Curves", BNL-325 (3rd Edition), Brookhaven National Laboratory, Upton, NY 11973, U.S.A. (1976).

20. S. A. Cox and P. R. Hanley, IEE Trans. Nucl. Sci. <u>18</u>, 108 (1971).

21. <u>Table of the Isotopes, 7th Edition</u>, ed. C. Michael Lederer and Virginia S. Shirley, John Wiley and Sons, Inc., New York (1978).

22. K. A. Weaver, J. D. Anderson, H. H. Barschall and J. C. Davis, Nucl. Sci. Eng. <u>52</u>, 35 (1973).

23. Donald L. Smith, "Neutron Dosimetry for Radiation Damage in Fission and Fusion Reactors," <u>Nuclear Cross Sections for Technology</u>, Proceedings of the International Conference on Nuclear Cross Sections for Technology, Knoxville Tennessee, 22-26 October 1979, NBS Special Publication 594, National Bureau of Standards, U.S. Department of Commerce, Washington D.C., USA, p. 285.

24. F. B. Hildebrand, <u>Methods of Applied Mathematics</u>, Prentice-Hall, Inc., Englewood Cliffs, NJ (1952).

APPENDIX

A FORTRAN program named UNFOLD has been written to enable the formalism described in Section II to be tested numerically. This program was written for a small computer, therefore the dimensions of the group arrays are rather small. This is not an inherent limitation of the program, so it could readily be expanded to utilize the available core space of a larger computer. Program UNFOLD provides the user with the option of iterating the solution although such a procedure is not recommended, as discussed in Section II. If there is iteration, all that is iterated is the group cross section itself. That is, σ' and N_{σ}' replace the apriori σ and N_{σ} for the subsequent calculation. The quantities A_o, N_{Ao}, Φ and N_{Φ} are untouched in this iteration procedure. The following list defines the relationship between the program's input and output parameters and quantities described in Section II:

$$M = m$$

$$N = n$$

$$AO(I) = a_{oi}$$

$$EAO(I) = [(N_{Ao})_{ii}]^{1/2}$$

$$CAO(I,J) = (N_{Ao})_{ij}/[(N_{Ao})_{ii}\ (N_{Ao})_{jj}]^{1/2}$$

$$E(J) = E_j$$

$$EE(J) = \Delta E_j$$

$$DE(J) = (E_{hj} - E_{\ell j})$$

$$FEPS(J) = f_{\varepsilon j}$$

$$CE(I,J) = (C_E)_{ij}$$

$$CEPS(I,J) = (C_\varepsilon)_{ij}$$

$$PHI(I,J) = \phi_{ij}$$

$$FN(I,J) = f_{\nu ij}$$

$$ETA(I,J) = n_{Eij}$$

$$SIGO(J) = \sigma_j$$

$$ESIGO(J) = [(N_\sigma)_{jj}]^{1/2}$$

$$CSIGO(I,J) = (N_\sigma)_{ij}/[(N_\sigma)_{ii}(N_{\sigma jj})]^{1/2}$$

$$ITR = \begin{cases} 0 & \text{do not iterate solution} \\ \\ 1 & \text{iterate solution} \end{cases}$$

$$NEXT = \begin{cases} 0 & \text{terminate iteration} \\ \\ 1 & \text{continue iteration} \end{cases}$$

NITR = order of specific iteration (zero designates first pass).

$$CHI2 = (\chi_m^2/m)$$

$$SIG(J) = \sigma'_j$$

$$ESIG(J) = [(N'_\sigma)_{jj}]^{1/2}$$

$$CSIG(I,J) = (N'_\sigma)_{ij}/[(N'_\sigma)_{ii}(N'_{\sigma jj})]^{1/2}$$

Subroutine MATINV inverts matrices. Subroutine JORDAN solves systems of linear equations using the Gauss-Jordan method. AVPRT is a printer control subroutine which is used for a specific computer. Here it acts as a dummy routine.

```
C       UNFOLD - CDC 1784 - D.L. SMITH - AP 314
C
        DIMENSION AO(20),EAO(20),CAO(20,20),PHI(20,30),FN(20,30),ETA(20,30
       1),FEPS(30),CEPS(30,30),E(30),EE(30),DE(30),CE(30,30),SIGO(30),ESIG
       20(30),CSIGO(30,30)
        DIMENSION V(20,20),W(20,20),C(20,30),U(20,30),A(20),SIG(30),ESIG(3
       10),CSIG(30,30)
C
C       INITIALIZATION AND CONTROL
C
 1000 WRITE(4,1001)
 1001 FORMAT(/6HUNFOLD)
        WRITE(4,1002)
 1002 FORMAT(/11HI/O DEVICES)
        WRITE(4,1003)
 1003 FORMAT(36H INPUT-IRD,PRINT-IWR,PUNCH-IPUN (3I2)/)
        READ(4,1004) IRD,IWR,IPUN
 1004 FORMAT(3I2)
        WRITE(4,1005)
 1005 FORMAT(22HITERATION OPTION-ITR (I1)/)
        READ(4,1006) ITR
 1006 FORMAT(I1)
        NITR=0
C
C       READ INPUT DATA ON UNIT IRD
C
        READ(IRD,1) M,N
    1 FORMAT(2I5)
        DO 2 I=1,M
    2 READ(IRD,3) AO(I),EAO(I)
    3 FORMAT(6E12.5)
        DO 4 I=1,M
    4 READ(IRD,3) (CAO(I,J),J=1,I)
        DO 5 I=1,M
        DO 5 J=1,I
    5 CAO(J,I)=CAO(I,J)
        DO 6 I=1,N
    6 READ(IRD,3) E(I),EE(I),DE(I),FEPS(I)
        DO 7 I=1,N
    7 READ(IRD,3) (CE(I,J),J=1,I)
        DO 8 I=1,N
        DO 8 J=1,I
    8 CE(J,I)=CE(I,J)
        DO 9 I=1,N
    9 READ(IRD,3) (CEPS(I,J),J=1,I)
        DO 10 I=1,N
        DO 10 J=1,I
   10 CEPS(J,I)=CEPS(I,J)
        DO 11 I=1,M
        DO 11 J=1,N
   11 READ(IRD,3) PHI(I,J),FN(I,J),ETA(I,J)
        DO 12 I=1,N
   12 READ(IRD,3) SIGO(I),ESIGO(I)
        DO 13 I=1,N
   13 READ(IRD,3) (CSIGO(I,J),J=1,I)
        DO 14 I=1,N
        DO 14 J=1,I
   14 CSIGO(J,I)=CSIGO(I,J)
C
C       CALCULATIONS
```

```
C
   20 CØNTINUE
      DØ 31 I=1,M
      DØ 30 J=1,N
   30 C(I,J)=SIGO(J)*PHI(I,J)
      DØ 31 I=1,M
      A(I)=0.0
      DØ 31 J=1,N
   31 A(I)=A(I)+C(I,J)
      DØ 32 I=1,M
      DØ 32 J=1,N
      U(I,J)=0.0
      DØ 32 L=1,N
   32 U(I,J)=U(I,J)+ESIGO(J)*ESIGO(L)*CSIGO(J,L)*C(I,L)/SIGO(J)/SIGO(L)
      DØ 35 I=1,M
      DØ 35 J=1,M
      V(I,J)=EAO(I)*EAO(J)*CAO(I,J)
      DØ 35 K=1,N
      V(I,J)=V(I,J)+C(I,K)*U(J,K)
      DØ 35 L=1,N
      RV=0.0
      IF(I.NE.J) GØ TØ 34
      IF(K.NE.L) GØ TØ 34
      RV=RV+FN(I,K)*FN(J,L)
   34 CØNTINUE
      RV=RV+CEPS(K,L)*FEPS(K)*FEPS(L)
      RV=RV+CE(K,L)*ETA(I,K)*ETA(J,L)*EE(K)*EE(L)/PHI(I,K)/PHI(J,L)
   35 V(I,J)=V(I,J)+C(I,K)*RV*C(J,L)
      CALL MATINV(V,W,NTEST,M)
      IF(NTEST.EQ.1) GØ TØ 39
      WRITE(4,38)
   38 FØRMAT(/10HNØ INVERSE)
      GØ TØ 1000
   39 CHI2=0.0
      DØ 40 I=1,M
      DØ 40 J=1,M
   40 CHI2=CHI2+(AO(I)-A(I))*W(I,J)*(AO(J)-A(J))
      CHI2=CHI2/FLØAT(M)
      DØ 42 J=1,N
      SUM=1.0
      DØ 41 I=1,M
      DØ 41 K=1,M
   41 SUM=SUM+U(I,J)*W(I,K)*(AO(K)-A(K))
   42 SIG(J)=SIGO(J)*SUM
      DØ 43 I=1,N
      DØ 43 J=1,N
      CSIG(I,J)=ESIGO(I)*ESIGO(J)*CSIGO(I,J)
      DØ 43 K=1,M
      DØ 43 L=1,M
   43 CSIG(I,J)=CSIG(I,J)-SIGO(I)*SIGO(J)*W(K,L)*U(K,I)*U(L,J)
      DØ 45 I=1,N
   45 ESIG(I)=SQRT(CSIG(I,I))
      DØ 46 I=1,N
      DØ 46 J=1,I
   46 CSIG(I,J)=CSIG(I,J)/ESIG(I)/ESIG(J)
C
C     PRINT ØUTPUT ØN UNIT IWR
C
      IF(IWR.EQ.9) CALL AVPRT
      WRITE(IWR,100) N,N,NITR,CHI2
  100 FØRMAT(/13HN,N,NITR,CHI2/3I5,E12.5)
```

```
      WRITE(IWR,101)
  101 FORMAT(13HE,DE,SIG,ESIG)
      DO 102 I=1,N
  102 WRITE(IWR,3) E(I),DE(I),SIG(I),ESIG(I)
      WRITE(IWR,103)
  103 FORMAT(4HCSIG)
      DO 104 I=1,N
  104 WRITE(IWR,3) (CSIG(I,J),J=1,I)
C
C     PUNCH OUTPUT ON UNIT IPUN IF IPUN.NE.0
C
      IF(IPUN.EQ.0) GO TO 300
      WRITE(IPUN,200) N,M,NITR,CHI2
  200 FORMAT(3I5,E12.5)
      DO 201 I=1,N
  201 WRITE(IPUN,3) E(I),DE(I),SIG(I),ESIG(I)
      DO 202 I=1,N
  202 WRITE(IPUN,3) (CSIG(I,J),J=1,I)
C
C     DECISION REGARDING ITERATION, CONTINUE IF ITR.NE.0 AND NEXT.NE.0
C
  300 CONTINUE
      IF(ITR.EQ.0) GO TO 1000
      WRITE(4,301)
  301 FORMAT(/9HNEXT (I2)/)
      READ(4,3010) NEXT
 3010 FORMAT(I2)
      IF(NEXT.EQ.0) GO TO 1000
      NITR=NITR+1
      DO 302 I=1,N
      SIGO(I)=SIG(I)
      ESIGO(I)=ESIG(I)
      DO 302 J=1,N
  302 CSIGO(I,J)=CSIG(I,J)
      GO TO 20
C
      END
      SUBROUTINE MATINV(D,Q,NTEST,NS)
      DIMENSION D(20,20),Q(20,20),E(20,21)
      IP = NS + 1
      BIG=0.0
      DO 555 I=1,NS
      DO 555 J=1,NS
      ABD =ABS(D(I,J))
      IF(ABD-BIG) 555,555,554
  554 BIG = ABD
  555 CONTINUE
      FACT = SQRT(BIG)
      I = 1
    1 IF(I-NS) 2,2,20
    2 J = 1
    3 IF(J-NS) 4,4,3
    4 K = 1
    5 IF(K-NS) 6,6,7
    6 E(J,K) = D(K,J)/FACT
      K = K+1
      GO TO 5
    7 J = J+1
      GO TO 3
    8 L = 1
    9 IF(L-NS) 10,10,14
```

```
10 IF(L-I) 11,13,11
11 E(L,IP) = 0.0
12 L = L+1
   GO TO 9
13 E(L,IP) = 1.0
   GO TO 12
14 CALL JORDAN(NS,E,NTEST)
   IF(NTEST) 15,15,16
15 RETURN
16 M = 1
17 IF(M-NS) 18,18,19
18 Q(I,M) = E(M,IP)/FACT
   M = M+1
   GO TO 17
19 I = I+1
   GO TO 1
20 RETURN
   END
   SUBROUTINE JORDAN(N,C,INDEX)
   DIMENSION B(20),C(20,21)
   K=1
 1 IF(K-N) 2,2,22
 2 IF(C(K,K)) 10,3,10
 3 L=K+1
 4 IF(L-N) 5,5,21
 5 IF(C(L,K)) 7,6,7
 6 L=L+1
   GO TO 4
 7 M=1
 8 IF(M-N-1) 9,9,2
 9 B(M)=C(K,M)
   C(K,M)=C(L,M)
   C(L,M)=B(M)
   M=M+1
   GO TO 8
10 J=N+1
11 IF(J-K) 13,12,12
12 C(K,J)=C(K,J)/C(K,K)
   J=J-1
   GO TO 11
13 I=1
14 IF(I-N) 16,16,15
15 K=K+1
   GO TO 1
16 IF(I-K) 18,17,18
17 I=I+1
   GO TO 14
18 II=N+1
19 IF(II-K) 17,20,20
20 C(I,II)=C(I,II)-C(I,K)*C(K,II)
   II=II-1
   GO TO 19
21 INDEX=0
   GO TO 23
22 INDEX=1
23 RETURN
   END
   SUBROUTINE AVPRT
   CONTINUE
   RETURN
   END
```